Supporting Information

Kinetics and Mechanism of Redox Processes of Pt/C and Pt_3Co/C Cathode Electrocatalysts in a Polymer Electrolyte Fuel Cell during an Accelerated Durability Test

Nozomu Ishiguro,[*,†,‡,§] *Sutasinee Kityakarn,*[‡,§,] *Oki Sekizawa,*[‖] *Tomoya Uruga,*[‖,▽] *Hirosuke Matsui,*[⊥,†] *Masahiro Taguchi,*[⊥,†] *Kensaku Nagasawa,*[‖] *Toshihiko Yokoyama,*[§] *and Mizuki Tada**[*,†,‡,⊥]

[†] Element Visualization Team, Materials Visualization Photon Science Group, RIKEN SPring-8 Center, 1-1-1 Koto, Sayo, Hyogo 679-5198, Japan.

[‡] Research Center for Materials Science (RCMS) & Integrated Research Consortium on Chemical Sciences (IRCCS), Nagoya University, Furo-Cho, Chikusa-ku, Nagoya, Aichi 464-8602, Japan.

[§] Institute for Molecular Science, 38 Nishigo-naka, Myodaiji, Okazaki, Aichi 444-8585, Japan.

[¶] Department of Chemistry, Faculty of Science, Kasetsart University, Bangkok 10903, Thailand.

[‖] Innovation Research Center for Fuel Cells, The University of Electro-Communications, 1-5-1 Chofugaoka, Chofu, Tokyo 182-8585, Japan.

[▽] Japan Synchrotron Radiation Research Institute, SPring-8, 1-1-1 Koto, Sayo, Hyogo 679-5198, Japan.

[⊥] Department of Chemistry, Graduate School of Science, Nagoya University, Furo-Cho, Chikusa-ku, Nagoya, Aichi 464-8602, Japan.

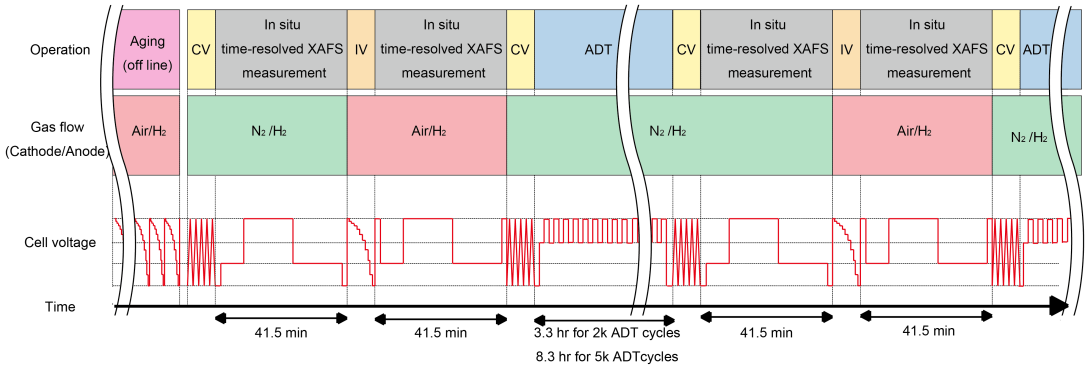

Figure S1. Schematic of protocol for in situ time-resolved XAFS measurements at SPring-8 BL36XU.

Details of Curve Fitting Analysis of STEM-EDS Line Profiles. Pt_3Co nanoparticles were treated as spheres, and their radii (r_1) were estimated by curve fitting $N_{tot}(x)$ of eq 1 in manuscript with a semicircular equation (eq SI1), convolved with a Gaussian.

$$N_{tot}^{fit}(x) = A\int_{-\infty}^{\infty}\frac{1}{\sqrt{\pi\sigma}}\exp\left(-\frac{x^2}{\sigma^2}\right)\cdot\sqrt{r_1^2-(x-\xi-x_1)^2}d\xi \quad \text{(SI1)}$$

Here, fitting parameters $A, \sigma, \xi,$ and x_1 were a proportional constant, the convolution width, an integration variable for the convolution, and the center x coordinate of the Pt_3Co particles, respectively. The line profiles of the Pt and Co atomic ratios were given by

$$R_{\mathrm{Pt}}(x) = N_{\mathrm{Pt}}(x)/N_{\mathrm{tot}}(x) \quad \text{(SI2)}$$

$$R_{\mathrm{Co}}(x) = N_{\mathrm{Co}}(x)/N_{\mathrm{tot}}(x) \quad \text{(SI3)}$$

and the thickness of the Pt-rich shells were estimated by curve fitting $R_{\mathrm{Co}}(x)$ with the following equation (eq SI4).

$$R_{\mathrm{Co}}^{fit}(x) = \begin{cases} R_{\mathrm{Co}}^{\mathrm{skin}} \ (x_1 - r_1 \le x < x_2 - r_2, x_2 + r_2 \le x < x_1 + r_1) \\ R_{\mathrm{Co}}^{\mathrm{skin}} + \frac{\left(R_{\mathrm{Co}}^{\mathrm{core}} - R_{\mathrm{Co}}^{\mathrm{skin}}\right)\sqrt{{r_2}^2-(x-x_2)^2}}{\sqrt{{r_1}^2-(x-x_1)^2}} \ (x_2 - r_2 \le x < x_2 + r_2) \end{cases} \quad \text{(SI4)}$$

In this model, inner Pt-Co alloy cores were treated as spheres with radius r_2, center x coordinate x_2, and uniform Co atomic ratio $R_{\mathrm{Co}}^{\mathrm{core}}$ (Figure S2). The remaining part of Pt_3Co nanoparticles was outer Pt-rich skin layers with uniform Co ratio of $R_{\mathrm{Co}}^{\mathrm{skin}}$ (Figure S2). Therefore, the average thickness of the Pt-rich skin layer of Pt_3Co/C nanoparticles, $\tau_{\mathrm{Pt-skin}}$, was defined as following (eq SI5).

$$\tau_{\mathrm{Pt-skin}} = r_1 - r_2 \quad \text{(SI5)}$$

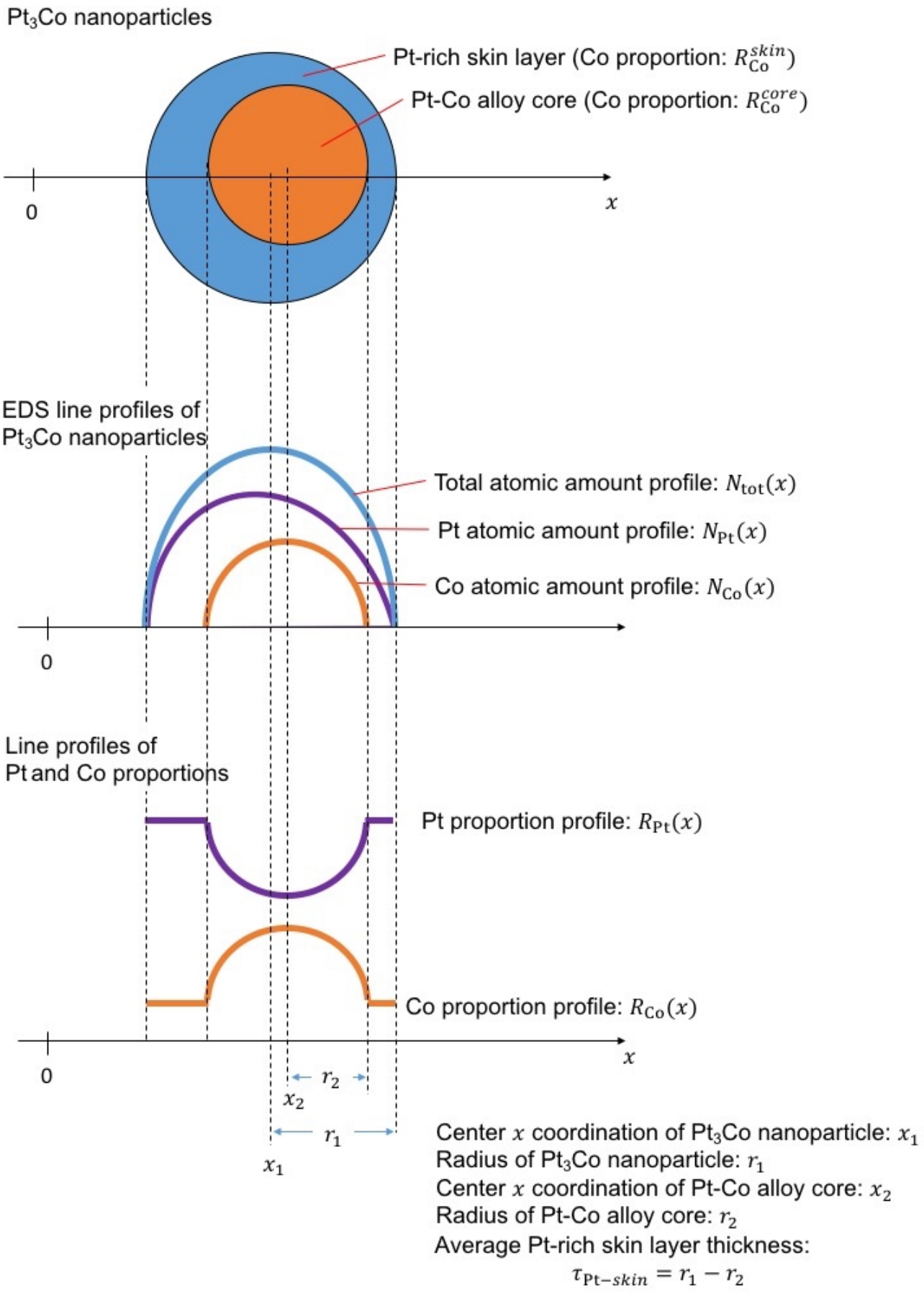

Figure S2. A schematic of Pt_3Co/C nanoparticle model, EDS line profile, and line profiles of Pt/Co proportions.

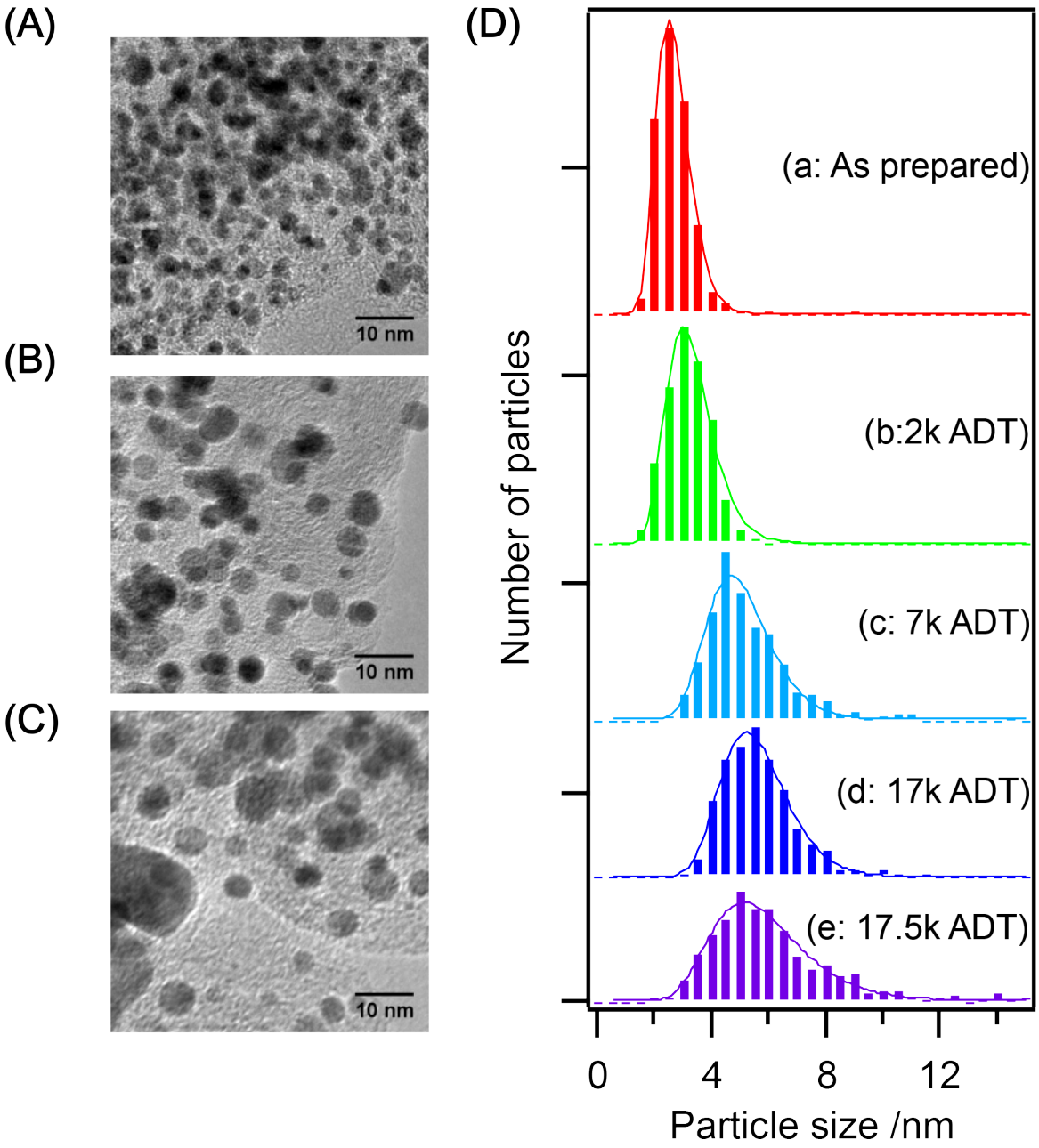

Figure S3. TEM images of Pt/C in (A) as-prepared MEA, (B) MEA after 7k ADT cycles, and (C) MEA after 17k ADT cycles. (D) Particle size distributions of Pt/C in (a) as-prepared MEA, (b) MEA after 2k ADT cycles, (c) MEA after 7k ADT cycles, (d) MEA after 17k ADT cycles, and (e) MEA after 17.5k ADT cycles. Curve fitting was performed with log-normal distribution:

$$N_{PSD}(D) = \frac{A}{\sigma x}\exp\left(-\frac{1}{2}\left(\frac{\ln(x/x_0)}{\sigma}\right)^2\right)$$

where x was particle size of the PSD bin, $N_{PSD}(x)$ was number of particles in the bin, x_0 was modal value of distribution, and σ was width of distribution.

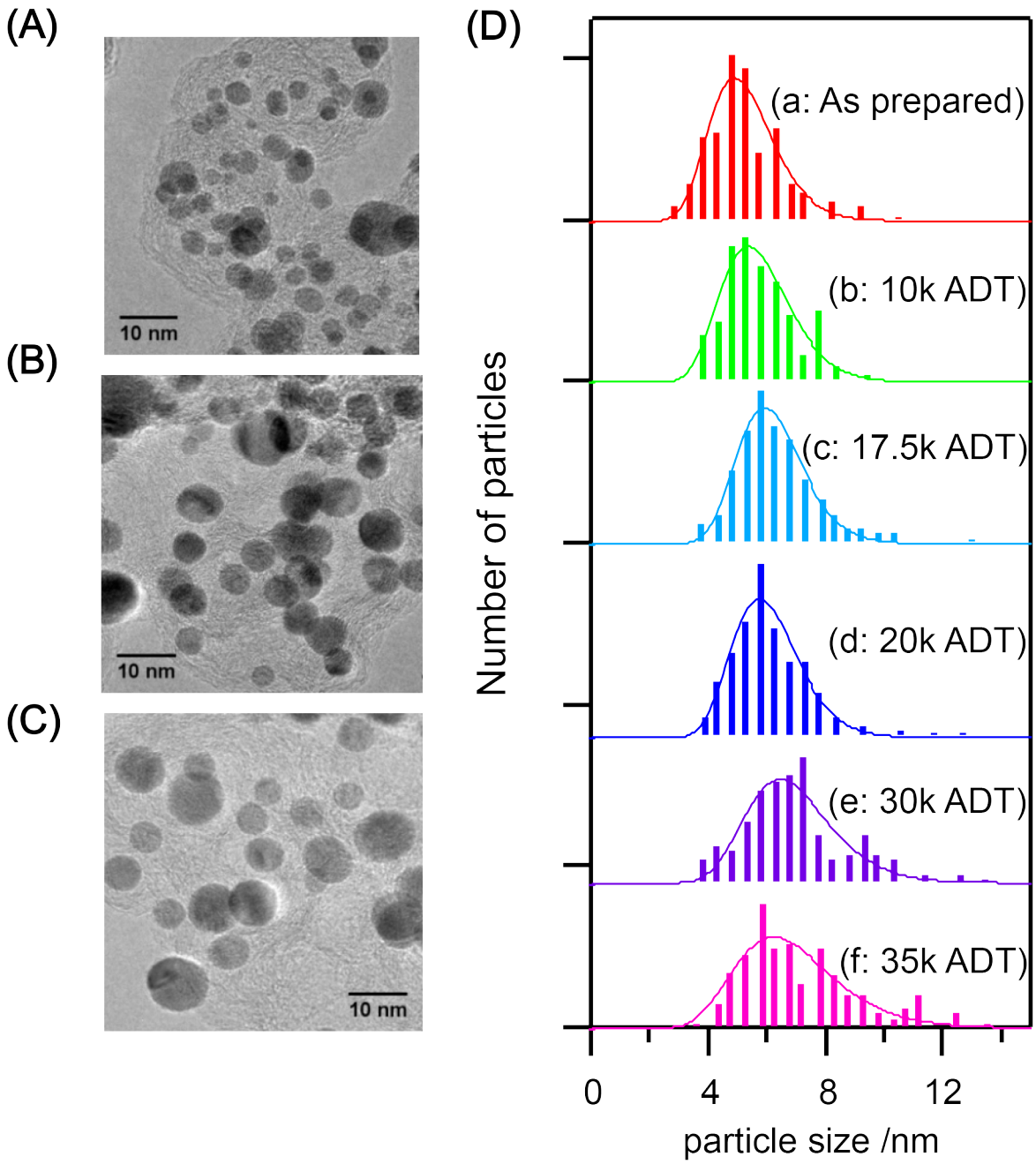

Figure S4. TEM images of Pt_3Co/C in (A) as-prepared MEA, (B) MEA after 17k ADT cycles, and (C) MEA after 35k ADT cycles. (D) Particle size distributions of Pt/C in (a) as-prepared MEA, (b) MEA after 10k ADT cycles, (c) MEA after 17.5k ADT cycles, (d) MEA after 20k ADT cycles, (e) MEA after 30k ADT cycles, and (f) MEA after 35k ADT cycles. Curve fitting was performed with log-normal distribution:

$$N_{PSD}(D) = \frac{A}{\sigma x}\exp\left(-\frac{1}{2}\left(\frac{\ln(x/x_0)}{\sigma}\right)^2\right)$$

where x was particle size of the PSD bin, $N_{PSD}(x)$ was number of particles in the bin, x_0 was modal value of distribution, and σ was width of distribution.

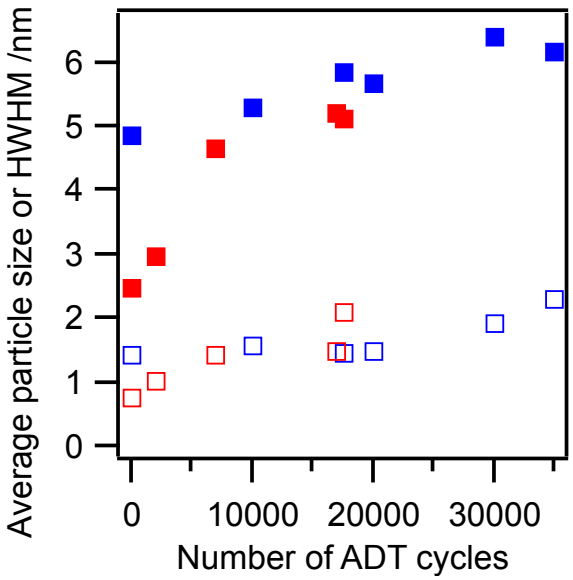

Figure S5. Changes in the particle size distribution of Pt/C (red) and Pt_3Co/C (blue) in the MEAs as a function of the number of ADT cycles. (■) average particle size in Figures S3 and S4; (□) HWHM of the particle size distribution in Figures S3 and S4.

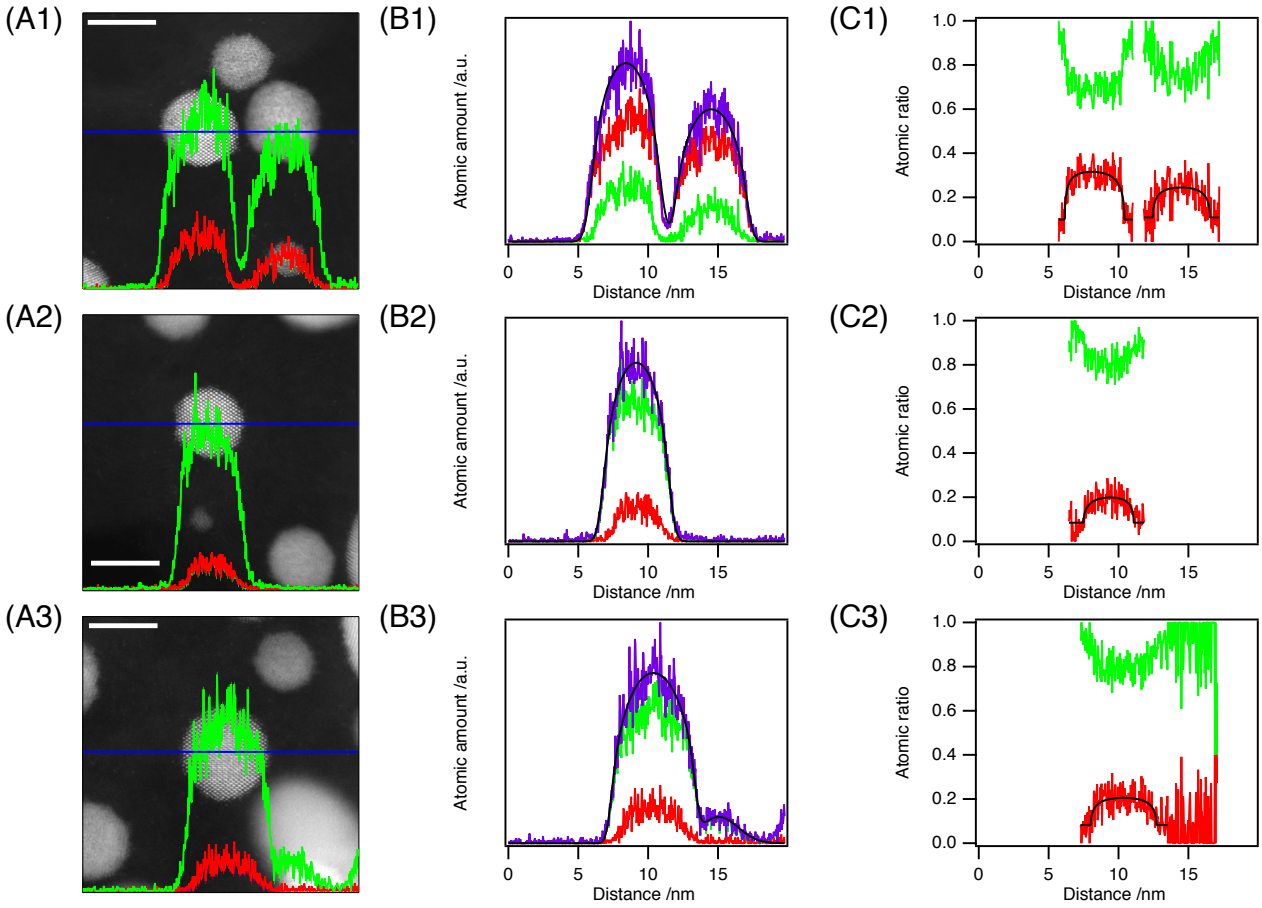

Figure S6. STEM-EDS line profile analyses of Pt_3Co nanoparticles (1) in as-prepared MEA and in MEAs after in situ XAFS measurements after (2) 17.5k ADT cycles and (3) 35k ADT cycles. (A) STEM-EDS line profiles of Pt Mα (red line) and Co Kα (green line) taken along the blue lines. Scale bars are 5 nm. (B) Line profiles of Pt, Co, and total (Pt + Co) atomic amounts calculated from the corresponding EDS line profiles in (A) (along the blue line). (C) Line profiles of the atomic ratios of Pt and Co for the particles in (A) (along the blue line). (Green lines) Pt; (red lines) Co; (purple lines) (Pt + Co); (black lines) curve-fitted lines.

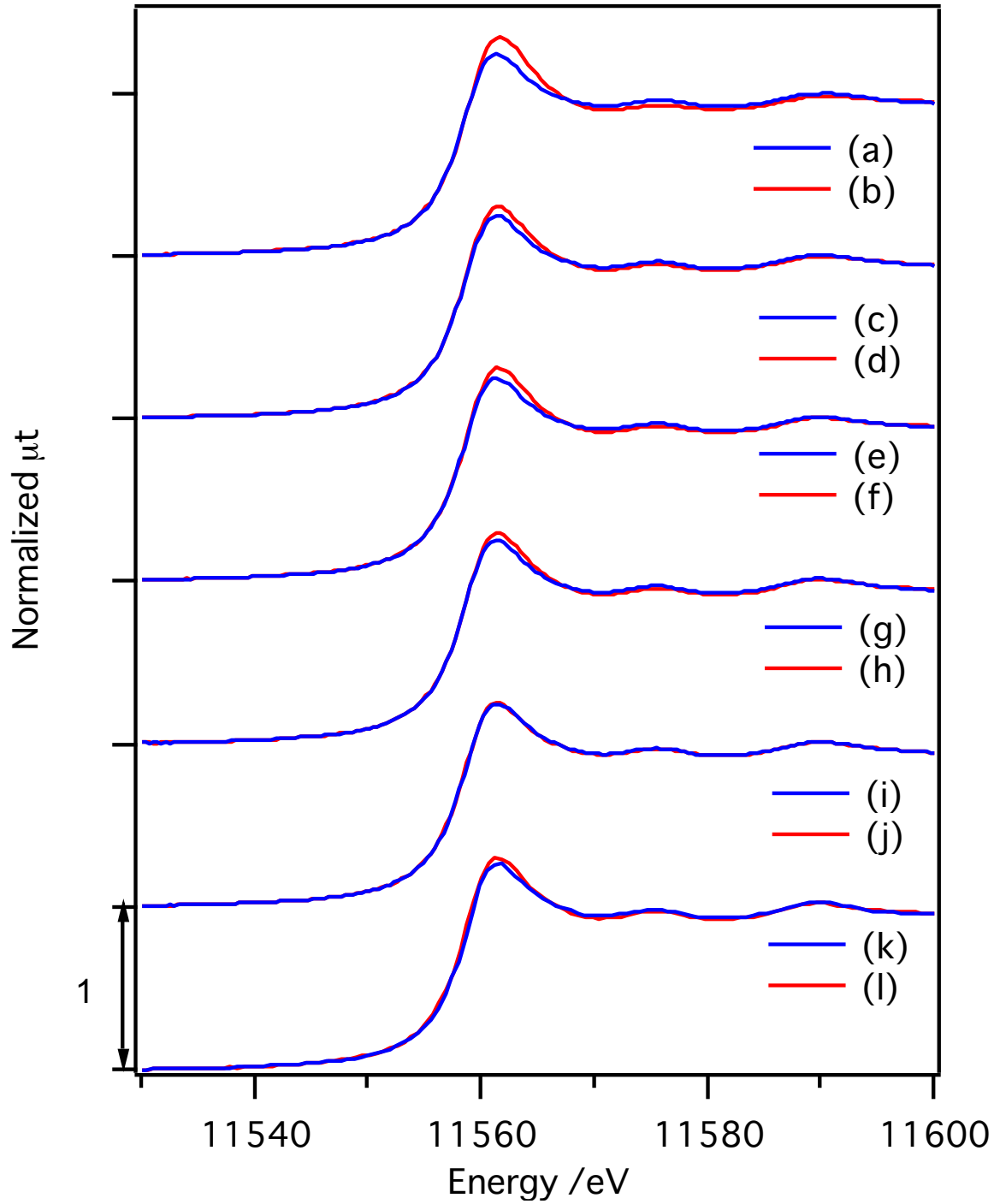

Figure S7. In situ Pt L_{III}-edge XANES of the Pt/C cathode catalyst in MEA during ADT. Pt/C (a) in as-prepared MEA, at 0.4 V, N_2; (b) in as-prepared MEA, at 1.0 V, N_2; (c) in MEA after 2k ADT cycles, at 0.4 V, N_2; (d) in MEA after 2k ADT cycles, at 1.0 V, N_2; (e) in MEA after 7k ADT cycles, at 0.4 V, N_2; (f) in MEA after 7k ADT cycles, at 1.0 V, N_2; (g) in MEA after 12k ADT cycles, at 0.4 V, N_2; (h) in MEA after 12k ADT cycles, at 1.0 V, N_2; (i) in MEA after 17k ADT cycles, at 0.4 V, N_2; (j) in MEA after 17k ADT cycles, at 1.0 V, N_2; (k) in MEA after 35k ADT cycles, at 0.4 V, N_2; and (l) in MEA after 35k ADT cycles, at 1.0 V, N_2.

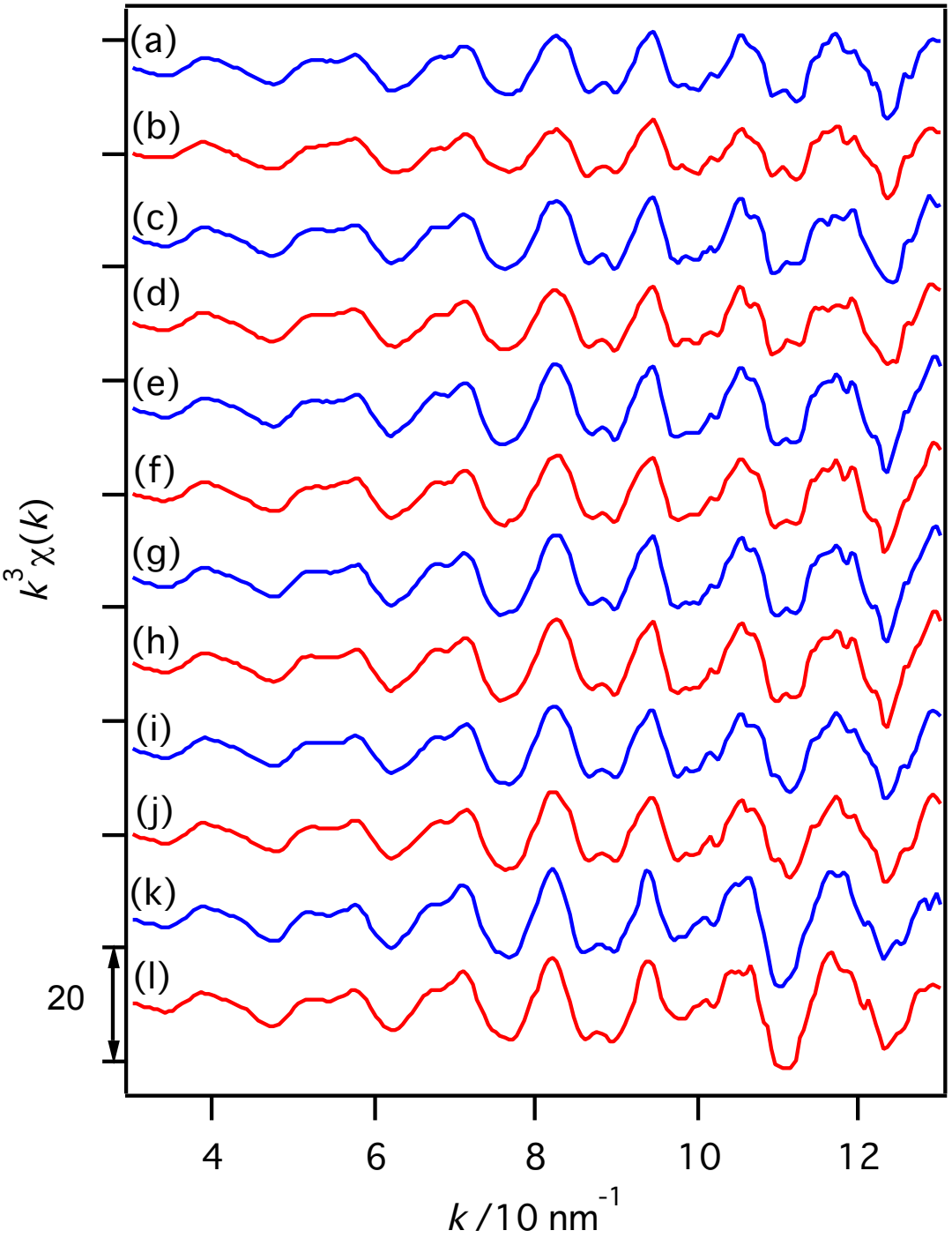

Figure S8. In situ Pt L_{III}-edge k^3-weighted EXAFS oscillations of the Pt/C cathode catalyst in MEA during ADT. Pt/C (a) in as-prepared MEA, at 0.4 V, N_2; (b) in as-prepared MEA, at 1.0 V, N_2; (c) in MEA after 2k ADT cycles, at 0.4 V, N_2; (d) in MEA after 2k ADT cycles, at 1.0 V, N_2; (e) in MEA after 7k ADT cycles, at 0.4 V, N_2; (f) in MEA after 7k ADT cycles, at 1.0 V, N_2; (g) in MEA after 12k ADT cycles, at 0.4 V, N_2; (h) in MEA after 12k ADT cycles, at 1.0 V, N_2; (i) in MEA after 17k ADT cycles, at 0.4 V, N_2; (j) in MEA after 17k ADT cycles, at 1.0 V, N_2; (k) in MEA after 35k ADT cycles, at 0.4 V, N_2; and (l) in MEA after 35k ADT cycles, at 1.0 V, N_2.

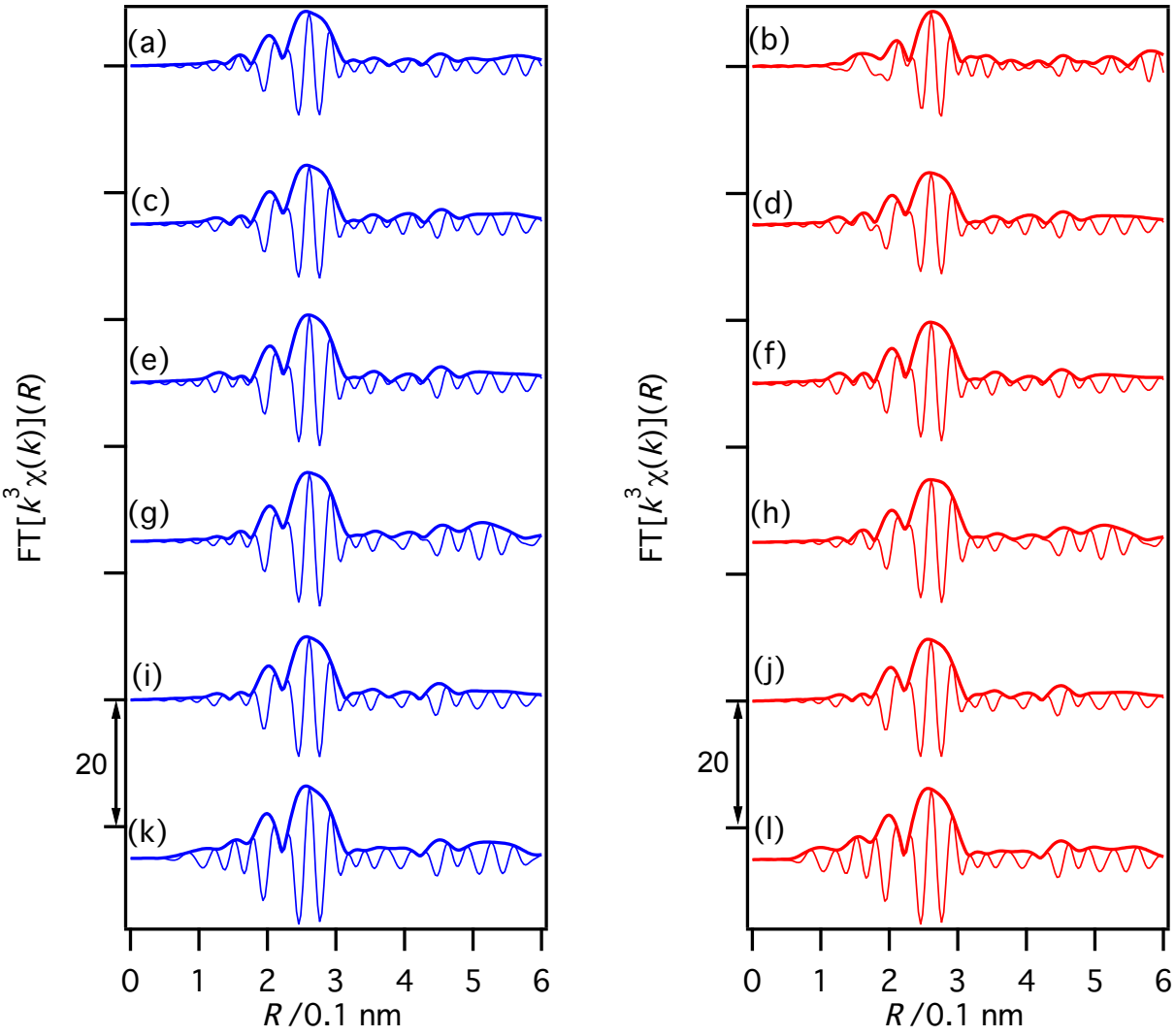

Figure S9. Fourier transforms of Figure S8 at k = 30−130 nm^{-1}. Pt/C (a) in as-prepared MEA, at 0.4 V, N_2; (b) in as-prepared MEA, at 1.0 V, N_2; (c) in MEA after 2k ADT cycles, at 0.4 V, N_2; (d) in MEA after 2k ADT cycles, at 1.0 V, N_2; (e) in MEA after 7k ADT cycles, at 0.4 V, N_2; (f) in MEA after 7k ADT cycles, at 1.0 V, N_2; (g) in MEA after 12k ADT cycles, at 0.4 V, N_2; (h) in MEA after 12k ADT cycles, at 1.0 V, N_2; (i) in MEA after 17k ADT cycles, at 0.4 V, N_2; (j) in MEA after 17k ADT cycles, at 1.0 V, N_2; (k) in MEA after 35k ADT cycles, at 0.4 V, N_2; and (l) in MEA after 35k ADT cycles, at 1.0 V, N_2.

Table S1 Curve-fitting Analysis of In Situ Pt L_{III}-edge EXAFS Oscillations of the Pt/C Cathode Catalyst in MEA during ADT

	Shell	CN	R /nm	ΔE_0 /eV	σ^2 /10^{-5} nm^2
(a) Pt/C in as-prepared MEA, at 0.4 V, N_2 (R_f=0.5%)	Pt-Pt	8.4 ± 0.6	0.275 ± 0.001	2.8 ± 0.4	6.8 ± 0.5
(b) Pt/C in as-prepared MEA, at 1.0 V, N_2 (R_f=0.9%)	Pt-Pt	6.3 ± 0.8	0.275 ± 0.001	2.8 ± 0.4	6.4 ± 0.8
	Pt-O	0.8 ± 0.3	0.202 ± 0.003	5 ± 4	4 ± 4
(c) Pt/C in MEA after 2k ADT cycles, at 0.4 V, N_2 (R_f=0.8%)	Pt-Pt	9.3 ± 0.5	0.275 ± 0.001	2.0 ± 0.5	7.0 ± 0.4
(d) Pt/C in MEA after 2k ADT cycles, at 1.0 V, N_2 (R_f=0.8%)	Pt-Pt	8.2 ± 0.7	0.275 ± 0.001	2.3 ± 0.6	6.9 ± 0.4
	Pt-O	0.5 ± 0.1	0.202	5	4
(e) Pt/C in MEA after 7k ADT cycles, at 0.4 V, N_2 (R_f=1.0%)	Pt-Pt	9.2 ± 0.5	0.275 ± 0.001	2.4 ± 0.5	6.1 ± 0.4
(f) Pt/C in MEA after 7k ADT cycles, at 1.0 V, N_2 (R_f=1.3%)	Pt-Pt	8.2 ± 0.7	0.275 ± 0.001	2.3 ± 0.7	6.1 ± 0.5
	Pt-O	0.3 ± 0.1	0.202	5	4
(g) Pt/C in MEA after 12k ADT cycles, at 0.4 V, N_2 (R_f=0.7%)	Pt-Pt	10.2 ± 0.5	0.276 ± 0.001	2.8 ± 0.7	6.5 ± 0.4
(h) Pt/C in MEA after 12k ADT cycles, at 1.0 V, N_2 (R_f=0.8%)	Pt-Pt	9.3 ± 0.6	0.276 ± 0.001	2.7 ± 0.6	6.5 ± 0.4
	Pt-O	0.3 ± 0.1	0.202	5	4
(i) Pt/C in MEA after 17k ADT cycles, at 0.4 V, N_2 (R_f=0.8%)	Pt-Pt	9.3 ± 0.5	0.275 ± 0.001	2.0 ± 0.5	6.7 ± 0.4
(j) Pt/C in MEA after 17k ADT cycles, at 1.0 V, N_2 (R_f=0.8%)	Pt-Pt	9.3 ± 0.6	0.275 ± 0.001	2.7 ± 0.6	6.8 ± 0.4
	Pt-O	-0.0 ± 0.1	0.202	5	4
(k) Pt/C in MEA after 35k ADT cycles, at 0.4 V, N_2 (R_f=2.6%)	Pt-Pt	10.1 ± 3.7	0.275	1.7 ± 0.6	6.2 ± 0.8
(l) Pt/C in MEA after 35k ADT cycles, at 1.0 V, N_2 (R_f=2.6 %)	Pt-Pt	10.1 ± 0.4	0.276	2.1 ± 0.3	6.3 ± 0.7
	Pt-O	0.1 ± 0.1	0.202	5	4

k = 30−130 nm^{-1}, R = 0.13−0.32 nm. R, ΔE_0, σ^2 of Pt-O in (d), (f), (h), (j), and (l) were fixed at the values in (b).

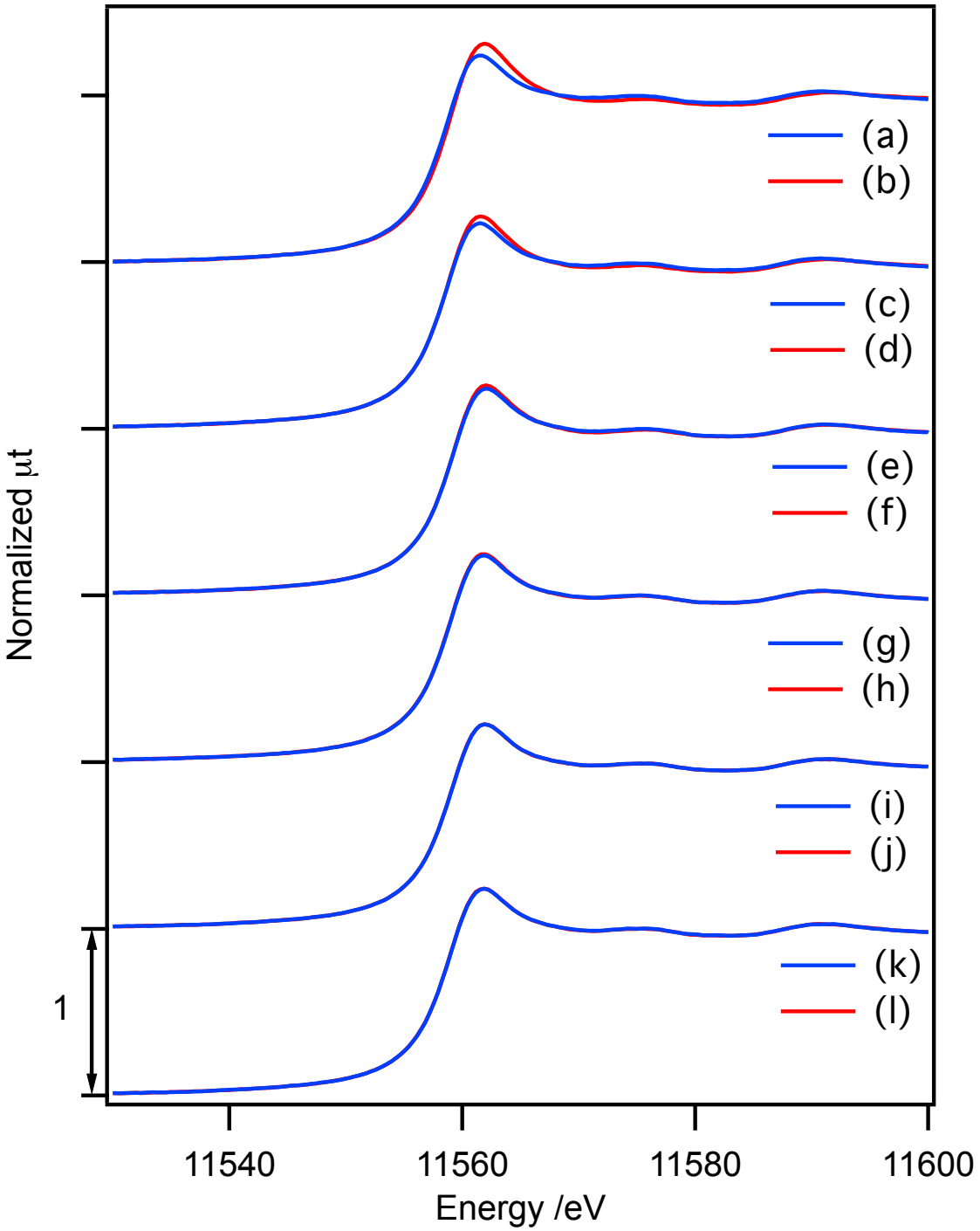

Figure S10. In situ Pt L_{III}-edge XANES of Pt_3Co/C cathode catalyst in MEA during ADT. Pt_3Co/C (a) in as-prepared MEA, at 0.4 V, N_2; (b) in as-prepared MEA, at 1.0 V, N_2; (c) in MEA after 5k ADT cycles, at 0.4 V, N_2; (d) in MEA after 5k ADT cycles, at 1.0 V, N_2; (e) in MEA after 10k ADT cycles, at 0.4 V, N_2; (f) in MEA after 10k ADT cycles, at 1.0 V, N_2; (g) in MEA after 20k ADT cycles, at 0.4 V, N_2; (h) in MEA after 20k ADT cycles, at 1.0 V, N_2; (i) in MEA after 30k ADT cycles, at 0.4 V, N_2; (j) in MEA after 30k ADT cycles, at 1.0 V, N_2; (k) in MEA after 35k ADT cycles, at 0.4 V, N_2; and (l) in MEA after 35k ADT cycles, at 1.0 V, N_2.

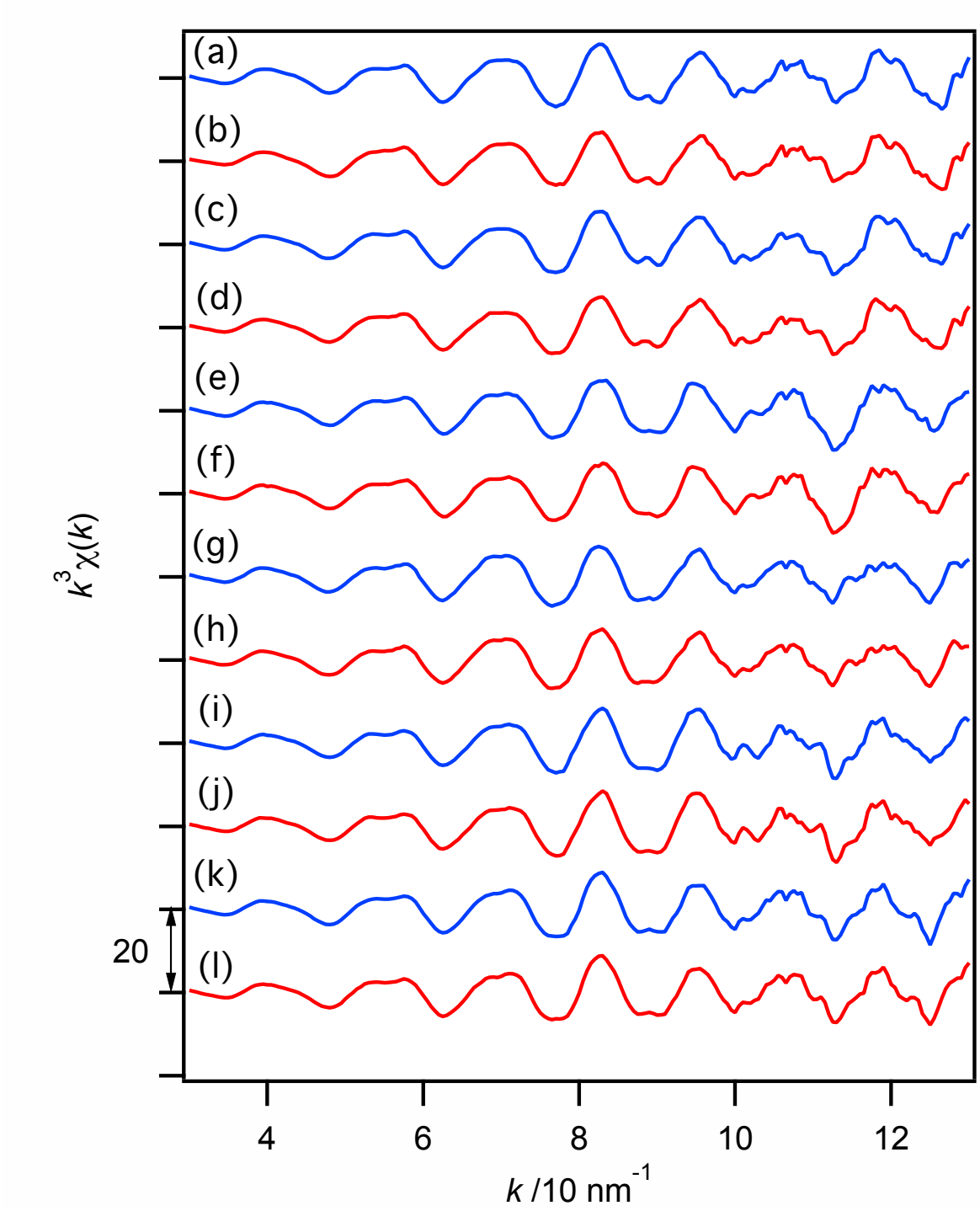

Figure S11. In situ Pt L_{III}-edge k^3-weighted EXAFS oscillations of the Pt_3Co/C cathode catalyst in MEA during ADT. Pt_3Co/C (a) in as-prepared MEA, at 0.4 V, N_2; (b) in as-prepared MEA, at 1.0 V, N_2; (c) in MEA after 5k ADT cycles, at 0.4 V, N_2; (d) in MEA after 5k ADT cycles, at 1.0 V, N_2; (e) in MEA after 10k ADT cycles, at 0.4 V, N_2; (f) in MEA after 10k ADT cycles, at 1.0 V, N_2; (g) in MEA after 20k ADT cycles, at 0.4 V, N_2; (h) in MEA after 20k ADT cycles, at 1.0 V, N_2; (i) in MEA after 30k ADT cycles, at 0.4 V, N_2; (j) in MEA after 30k ADT cycles, at 1.0 V, N_2; (k) in MEA after 35k ADT cycles, at 0.4 V, N_2; and (l) in MEA after 35k ADT cycles, at 1.0 V, N_2.

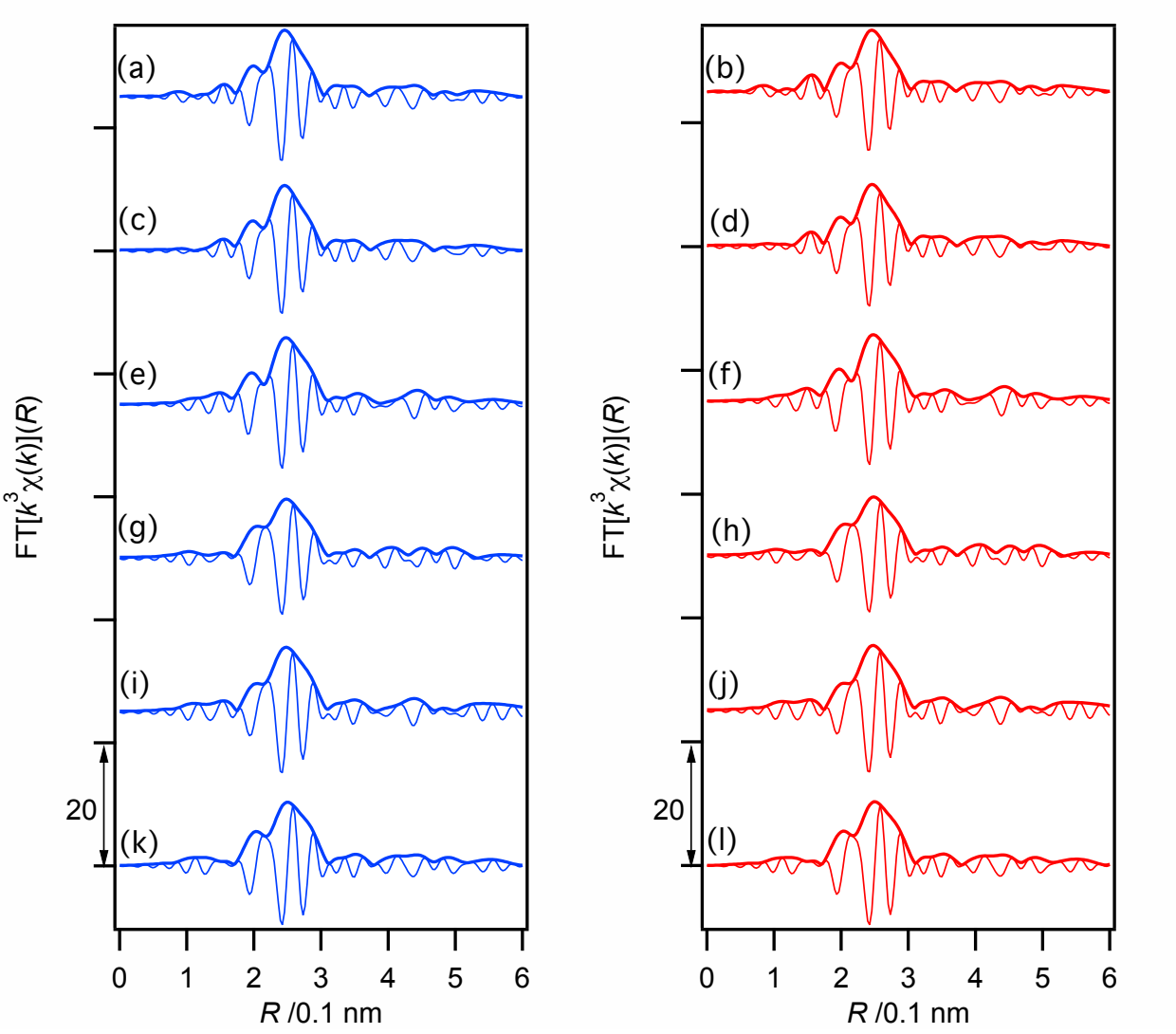

Figure S12. Fourier transforms of Figure S11 at k = 30−130 nm^{-1}. Pt_3Co/C (a) in as-prepared MEA, at 0.4 V, N_2; (b) in as-prepared MEA, at 1.0 V, N_2; (c) in MEA after 5k ADT cycles, at 0.4 V, N_2; (d) in MEA after 5k ADT cycles, at 1.0 V, N_2; (e) in MEA after 10k ADT cycles, at 0.4 V, N_2; (f) in MEA after 10k ADT cycles, at 1.0 V, N_2; (g) in MEA after 20k ADT cycles, at 0.4 V, N_2; (h) in MEA after 20k ADT cycles, at 1.0 V, N_2; (i) in MEA after 30k ADT cycles, at 0.4 V, N_2; (j) in MEA after 30k ADT cycles, at 1.0 V, N_2; (k) in MEA after 35k ADT cycles, at 0.4 V, N_2; and (l) in MEA after 35k ADT cycles, at 1.0 V, N_2.

Table S2 Curve-fitting Analysis of In Situ Pt L_{III}-edge EXAFS Oscillations of the Pt_3Co/C Cathode Catalyst in MEA during ADT

	Shell	CN	*R* /nm	ΔE_0 /eV	σ^2 /10^{-5} nm^2
(a) Pt_3Co/C in as-prepared MEA, 0.4 V, N_2 (R_f=1.4%)	Pt-Pt	5.4 ± 2.5	0.270 ± 0.001	-0 ± 4	5 ± 2
	Pt-Co	3.8 ± 2.1	0.266 ± 0.004	2 ± 6	13 ± 5
(b) Pt_3Co/C in as-prepared MEA, 1.0 V, N_2 (R_f=1.2%)	Pt-Pt	5.0 ± 2.5	0.270 ± 0.001	- 0± 4	5 ± 2
	Pt-Co	3.8 ± 2.1	0.267 ± 0.005	3 ± 6	1 ± 5
	Pt-O	0.4 ± 0.3	1.98	-1	1.00
(c) Pt_3Co/C in MEA after 5k ADT cycles, at 0.4 V, N_2 (R_f=1.4%)	Pt-Pt	6.1 ± 2.7	0.270 ± 0.001	-1 ± 4	5 ± 2
	Pt-Co	3.5 ± 2.1	0.267 ± 0.005	3 ± 7	13 ± 5
(d) Pt_3Co/C in MEA after 5k ADT cycles, at 1.0 V, N_2 (R_f=1.4%)	Pt-Pt	5.1 ± 2.8	0.270 ± 0.002	-1 ± 5	5 ± 2
	Pt-Co	3.7 ± 2.4	0.267 ± 0.006	3 ± 7	13 ± 6
	Pt-O	0.5 ± 0.1	1.98	-1	1.00
(e) Pt_3Co/C in MEA after 10k ADT cycles, at 0.4 V, N_2 (R_f=2.8%)	Pt-Pt	8.1 ± 0.5	0.270 ± 0.001	-0 ± 4	6.5 ± 2
	Pt-Co	3.1 ± 0.5	0.266	2 ± 7	16 ± 1
(f) Pt_3Co/C in MEA after 10k ADT cycles, at 1.0 V, N_2 (R_f=2.3%)	Pt-Pt	8.1 ± 3.4	0.270 ± 0.001	-0 ± 4	7 ± 2
	Pt-Co	4.2 ± 5.3	0.266	3 ± 6	20 ± 2
	Pt-O	-0.3 ± 0.4	1.98	-1	1.00
(g) Pt_3Co/C in MEA after 20k ADT cycles, at 0.4 V, N_2 (R_f=0.6%)	Pt-Pt	8.9 ± 2.0	0.273 ± 0.001	2 ± 2	8 ± 1
	Pt-Co	2.3 ± 1.1	0.265 ± 0.003	1 ± 5	10 ± 3
(h) Pt_3Co/C in MEA after 20k ADT cycles, at 1.0 V, N_2 (R_f=0.5%)	Pt-Pt	8.6 ± 2.1	0.273 ± 0.001	2 ± 2	8 ± 1
	Pt-Co	2.3 ±1.2	0.264 ± 0.003	1 ± 5	10 ± 4
	Pt-O	-0.0 ± 0.2	1.98	-1	1.00
(i) Pt_3Co/C in MEA after 30k ADT cycles, at 0.4 V, N_2 (R_f=1.6%)	Pt-Pt	8.3 ± 3.2	0.272 ± 0.001	3 ± 3	7 ± 2
	Pt-Co	1.4 ± 1.5	0.265 ± 0.005	1 ± 10	6 ± 6
(j) Pt_3Co/C in MEA after 30k ADT cycles, at 1.0 V, N_2 (R_f=1.3%)	Pt-Pt	8.4 ± 3.4	0.272 ± 0.001	3 ± 4	7 ± 2
	Pt-Co	1.4 ± 1.5	0.265 ± 0.005	2 ± 10	6 ± 6
	Pt-O	0.2 ± 0.3	1.98	-1	1.00
(k) Pt_3Co/C in MEA after 35k ADT cycles, at 0.4 V, N_2 (R_f=0.8%)	Pt-Pt	8.0 ± 2.3	0.272 ± 0.001	3 ± 3	7 ± 1
	Pt-Co	2.3 ± 1.6	0.262 ± 0.004	-3 ± 7	11 ± 5
(l) Pt_3Co/C in MEA after 35k ADT cycles, at 1.0 V, N_2 (R_f=0.6%)	Pt-Pt	7.5 ± 2.2	0.272 ± 0.001	3 ±3	6 ± 1
	Pt-Co	2.4 ± 1.5	0.262 ± 0.004	-2 ± 6	10 ± 4
	Pt-O	-0.2 ± 0.2	1.98	-1	1.00

k = 30−130 nm^{-1}, R = 0.13−0.32 nm. R, ΔE_0, σ^2 of Pt-O in (b), (d), (f), (h), (j), and (l) were fixed at the values in ref. 28. R values of Pt-Co in (e) and (f) were fixed at the value in (a).

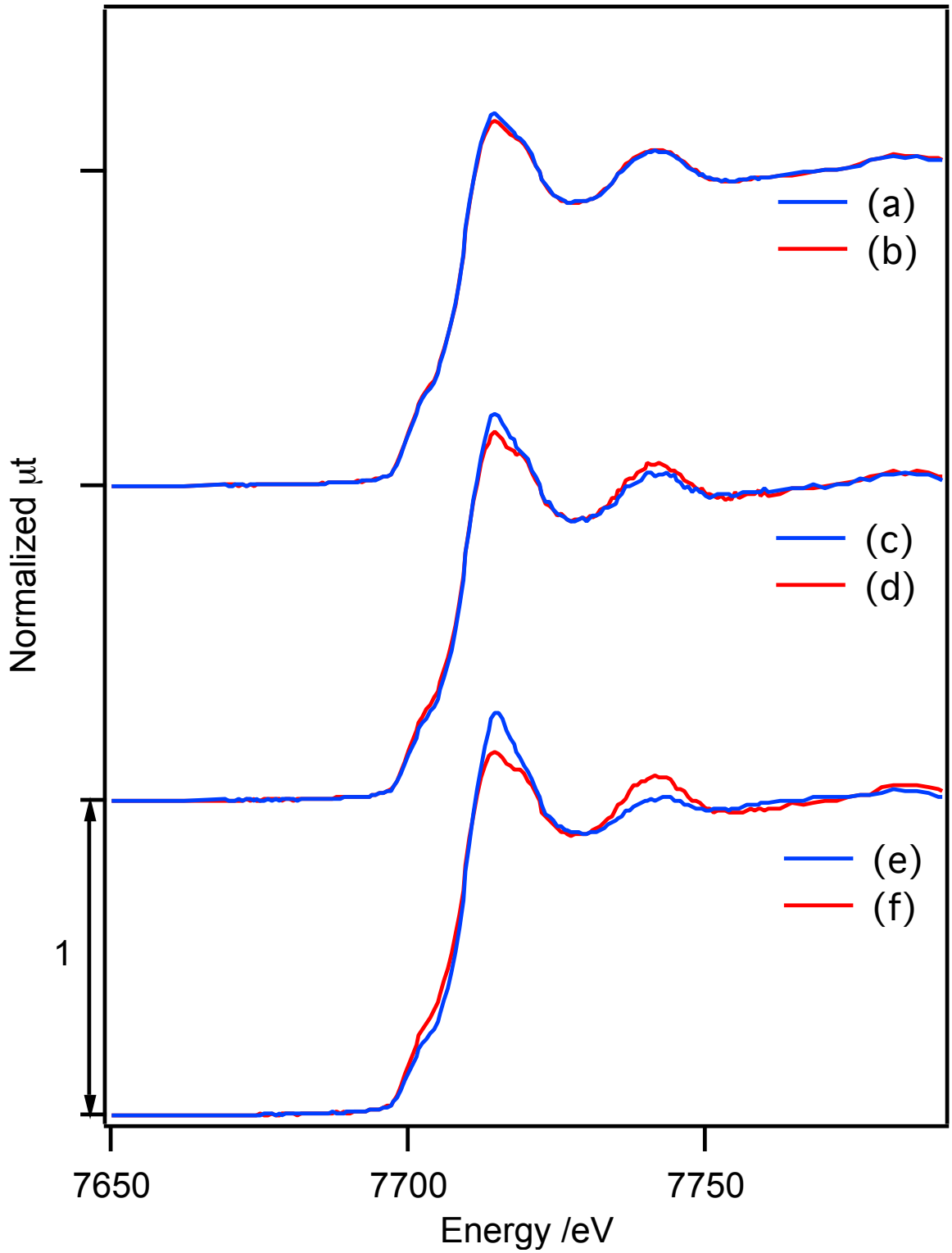

Figure S13. In situ Co K-edge XANES of Pt_3Co/C cathode catalyst in MEA during ADT. Pt_3Co/C (a) in as-prepared MEA, at 0.4 V, N_2; (b) in as-prepared MEA, at 1.0 V, N_2; (c) in MEA after 10k ADT cycles, at 0.4 V, N_2; (d) in MEA after 10k ADT cycles at 1.0 V, N_2; (e) in MEA after 35k ADT cycles at 0.4 V, N_2; and (f) in MEA after 35k ADT cycles, at 1.0 V, N_2.

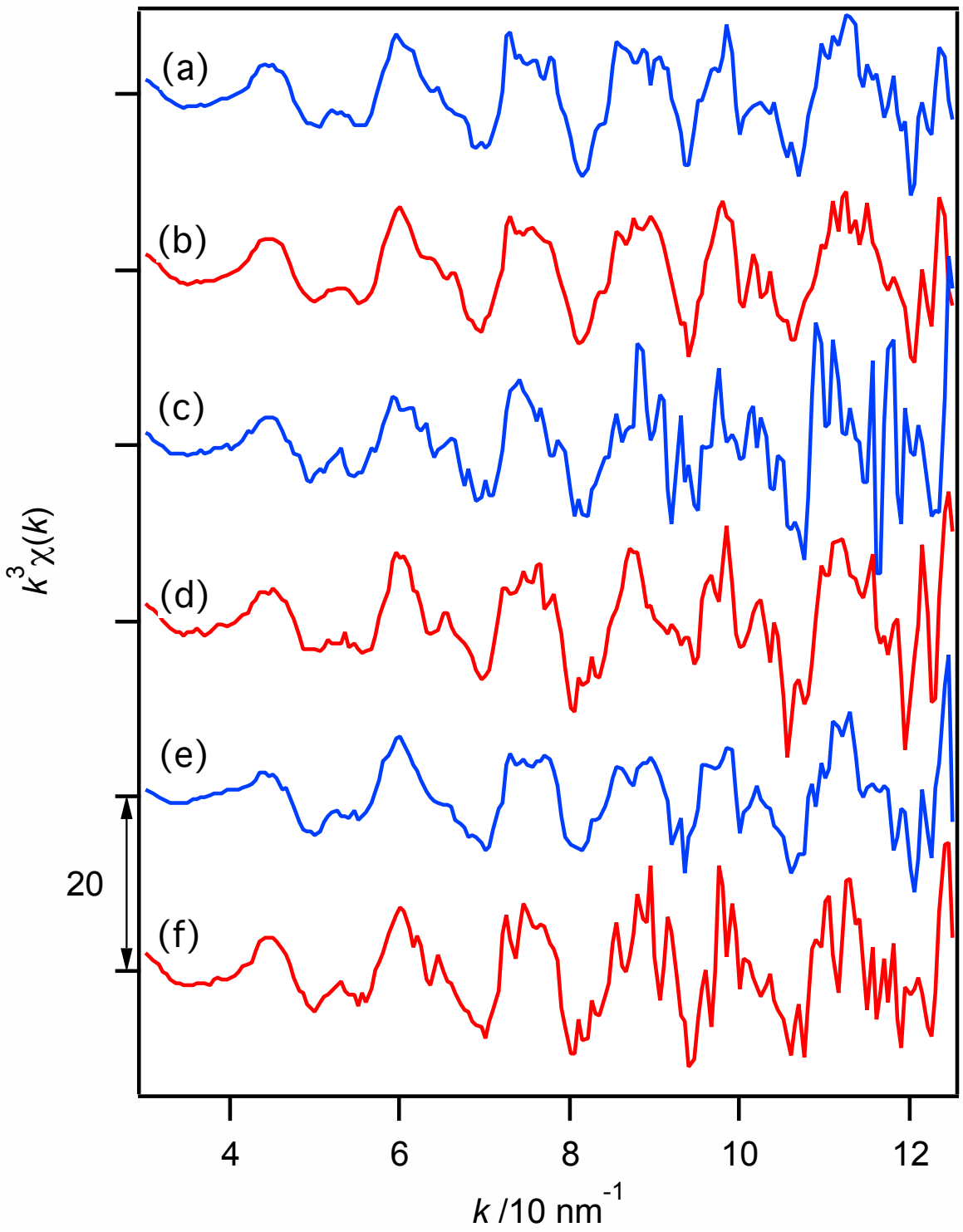

Figure S14. In situ Co K-edge k^3-weighted EXAFS oscillations of Pt_3Co/C cathode catalysts. Pt_3Co/C (a) in as-prepared MEA, at 0.4 V, N_2; (b) in as-prepared MEA, at 1.0 V, N_2; (c) in MEA after 10k ADT cycles, at 0.4 V, N_2; (d) in MEA after 10k ADT cycles at 1.0 V, N_2; (e) in MEA after 35k ADT cycles at 0.4 V, N_2; and (f) in MEA after 35k ADT cycles, at 1.0 V, N_2.

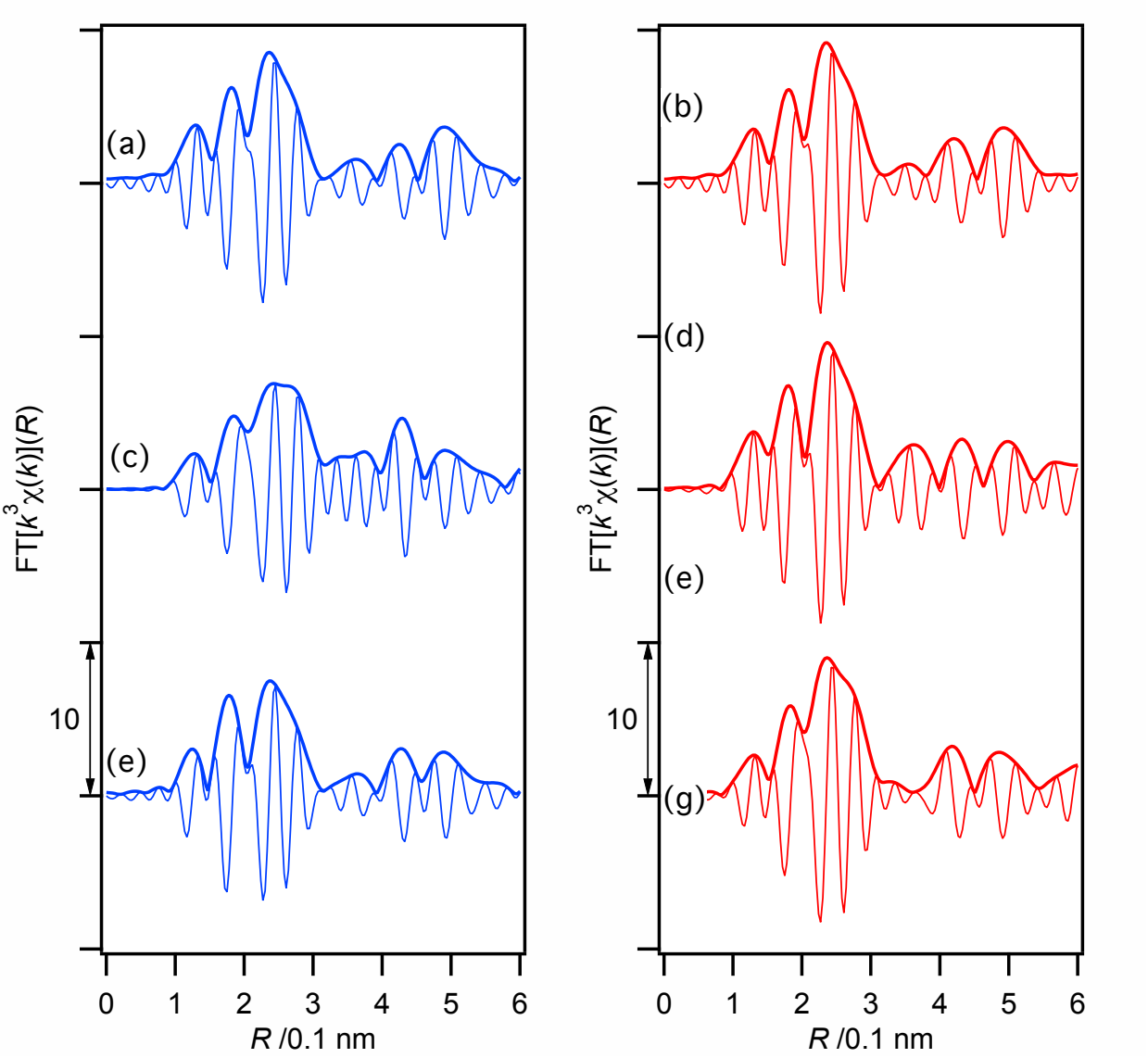

Figure S15. Fourier transforms of Figure S14 at k = 30−120 nm^{-1}. Pt_3Co/C (a) in as-prepared MEA, at 0.4 V, N_2; (b) in as-prepared MEA, at 1.0 V, N_2; (c) in MEA after 10k ADT cycles, at 0.4 V, N_2; (d) in MEA after 10k ADT cycles at 1.0 V, N_2; (e) in MEA after 35k ADT cycles at 0.4 V, N_2; and (f) in MEA after 35k ADT cycles, at 1.0 V, N_2.

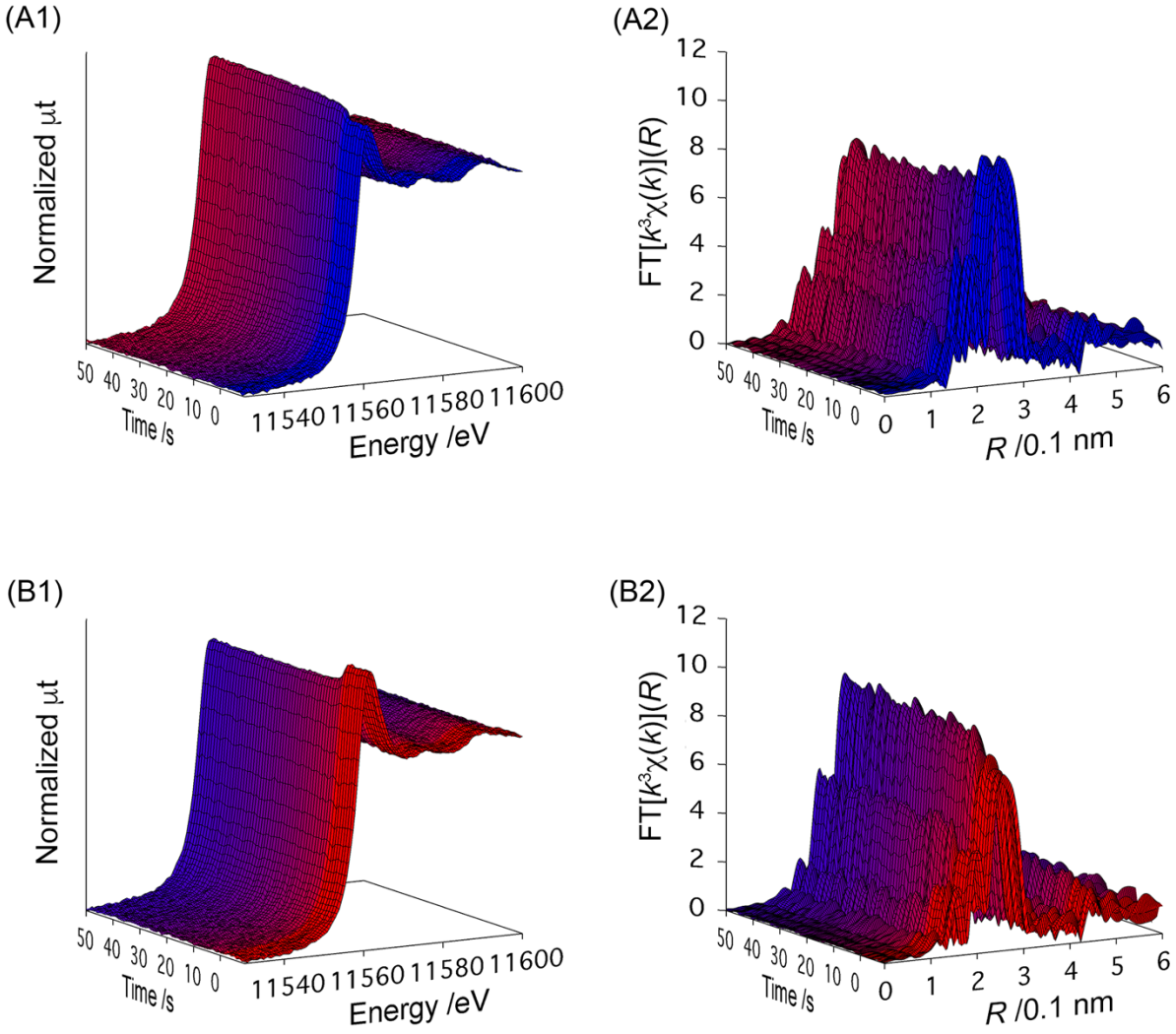

Figure S16. Series of in situ time-resolved Pt L_{III}-edge QXAFS spectra for Pt/C in as-prepared MEA. (1) Series of in situ time-resolved Pt L_{III}-edge XANES spectra and (2) series of in situ time-resolved Pt L_{III}-edge k^3-weighted EXAFS Fourier transforms at k = 30–130 nm^{-1} for the voltage cycling of (A) 0.4 → 1.0 V and (B) 1.0 → 0.4 V in N_2.

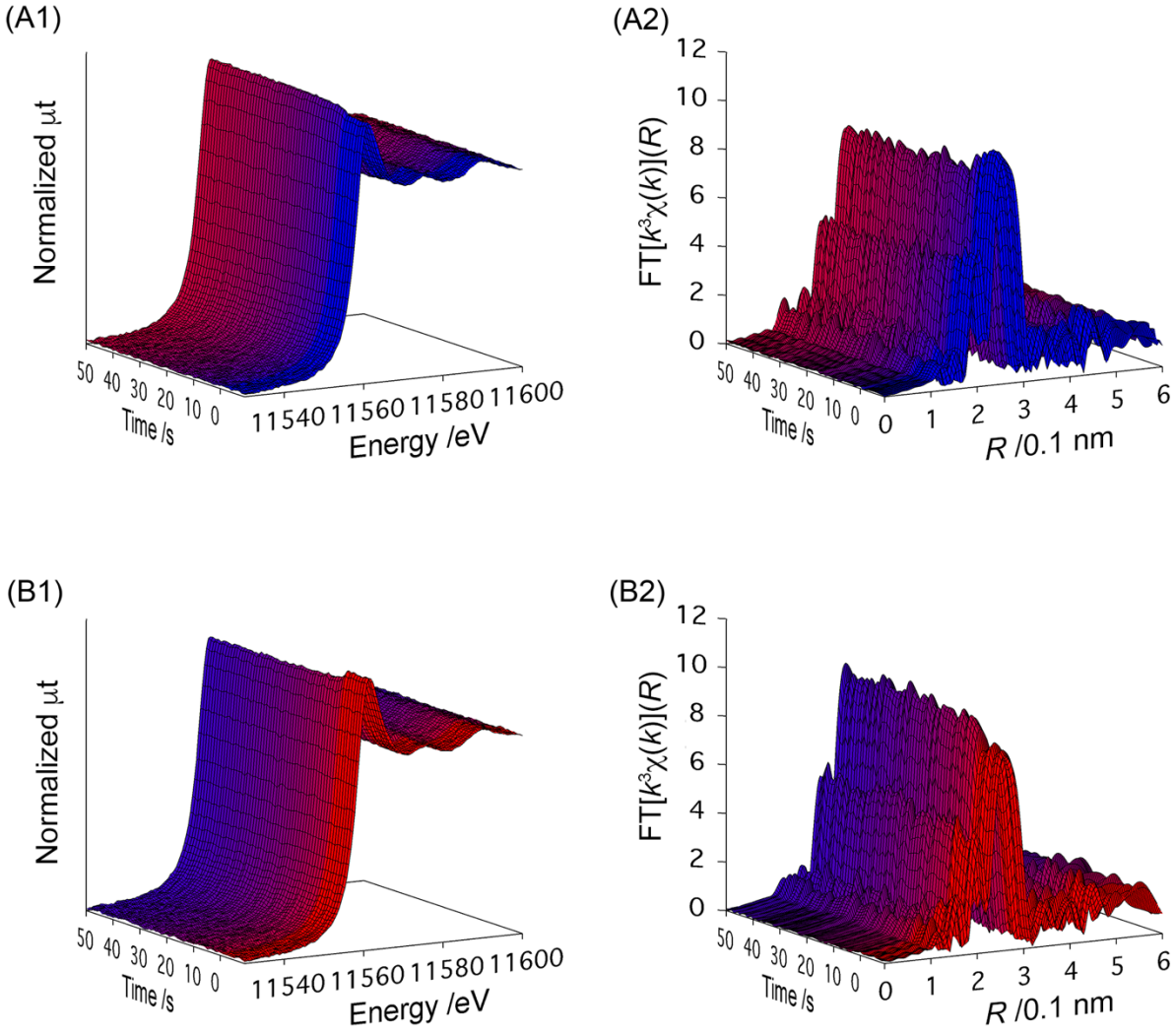

Figure S17. Series of in situ time-resolved Pt L_{III}-edge QXAFS spectra for Pt/C in MEA after 2k ADT cycles. (1) Series of in situ time-resolved Pt L_{III}-edge XANES spectra and (2) series of in situ time-resolved Pt L_{III}-edge k^3-weighted EXAFS Fourier transforms at k = 30–130 nm^{-1} for voltage cycling of (A) 0.4 → 1.0 V and (B) 1.0 → 0.4 V in N_2.

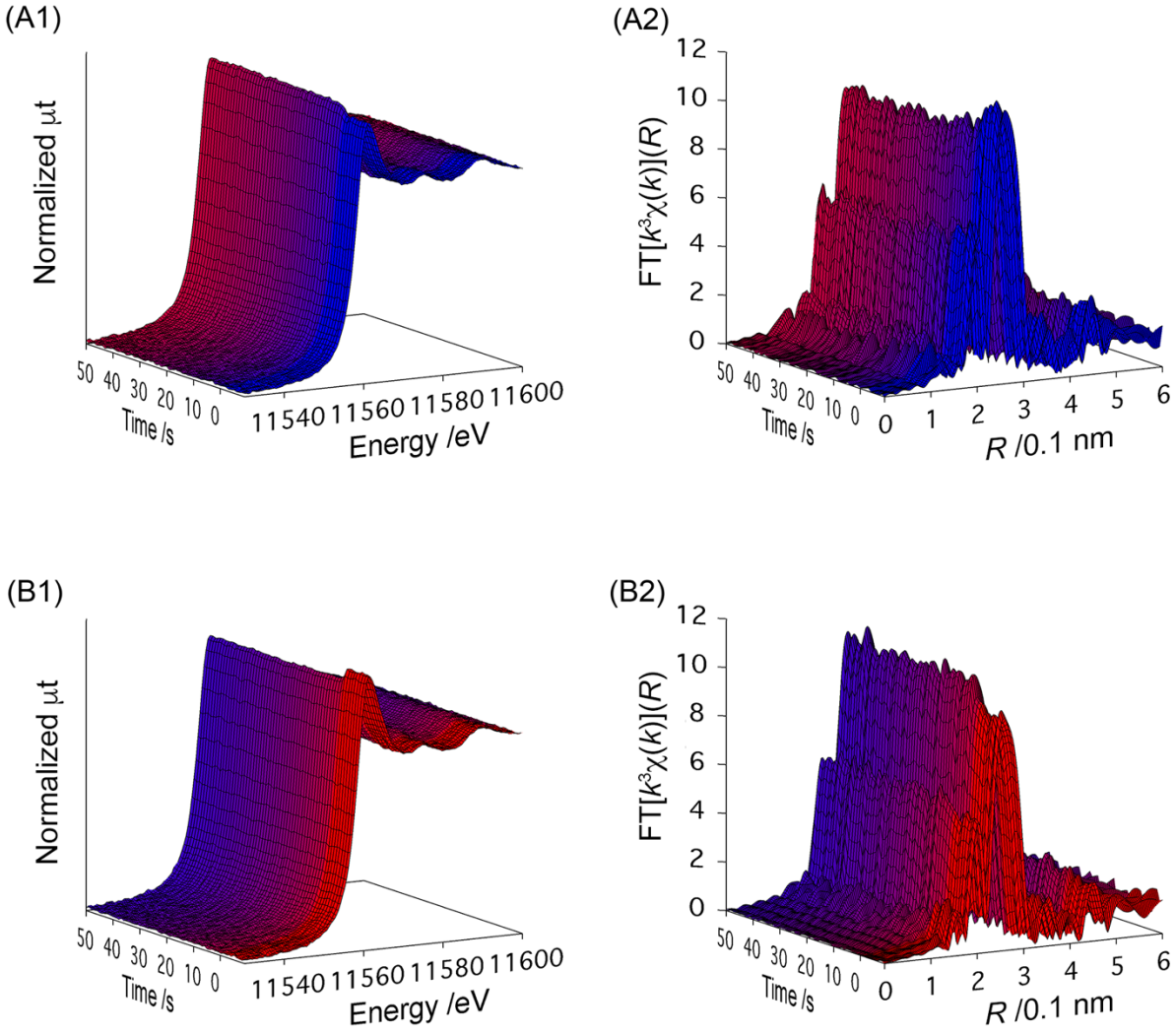

Figure S18. Series of in situ time-resolved Pt L_{III}-edge QXAFS spectra for Pt/C in MEA after 7k ADT cycles. (1) Series of in situ time-resolved Pt L_{III}-edge XANES spectra and (2) series of in situ time-resolved Pt L_{III}-edge k^3-weighted EXAFS Fourier transforms at k = 30–130 nm^{-1} for voltage cycling of (A) 0.4 → 1.0 V and (B) 1.0 → 0.4 V in N_2.

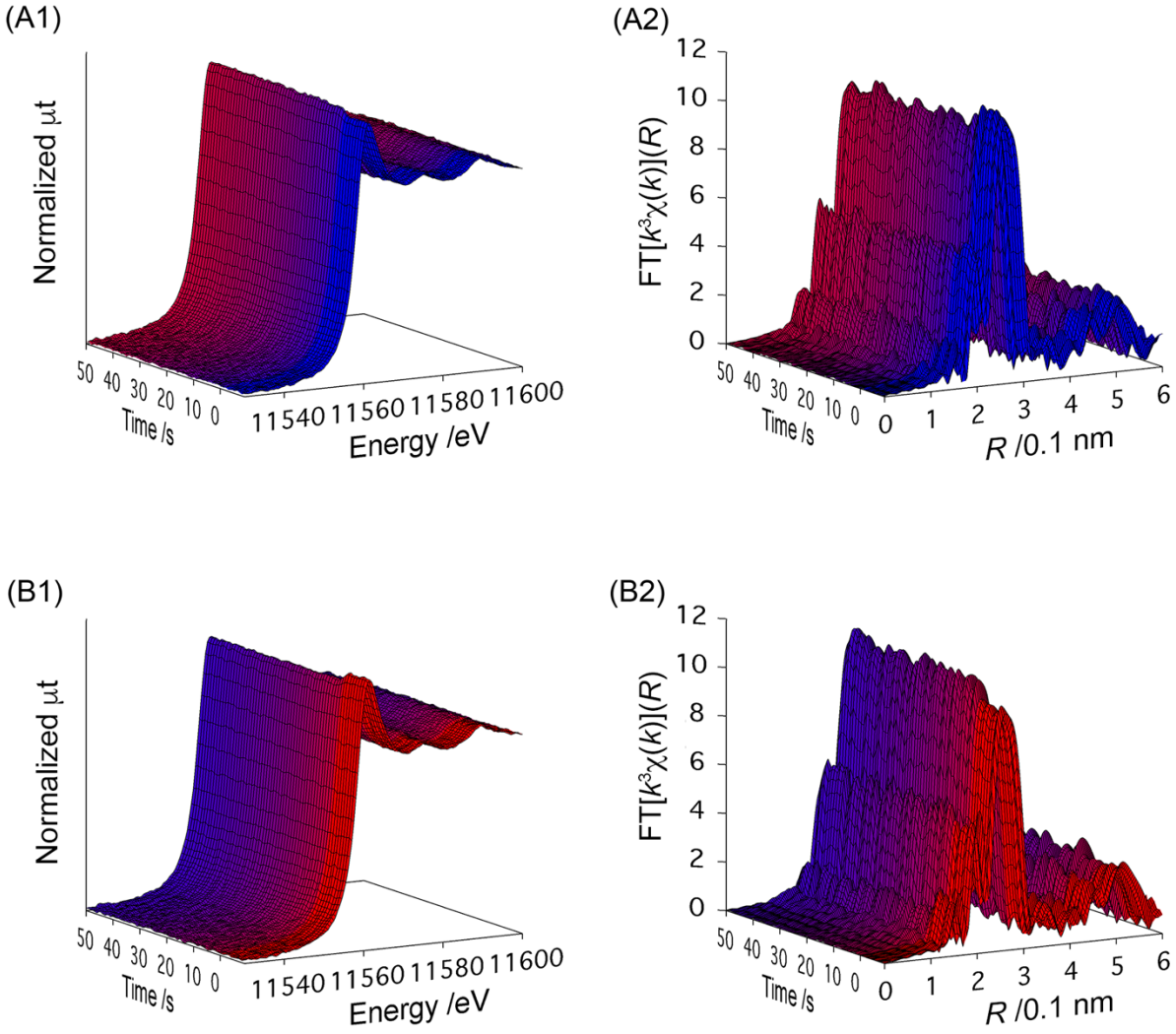

Figure S19. Series of in situ time-resolved Pt L_{III}-edge QXAFS spectra for Pt/C in MEA after 12k ADT cycles. (1) Series of in situ time-resolved Pt L_{III}-edge XANES spectra and (2) series of in situ time-resolved Pt L_{III}-edge k^3-weighted EXAFS Fourier transforms at k = 30–130 nm^{-1} for voltage cycling of (A) 0.4 → 1.0 V and (B) 1.0 → 0.4 V in N_2.

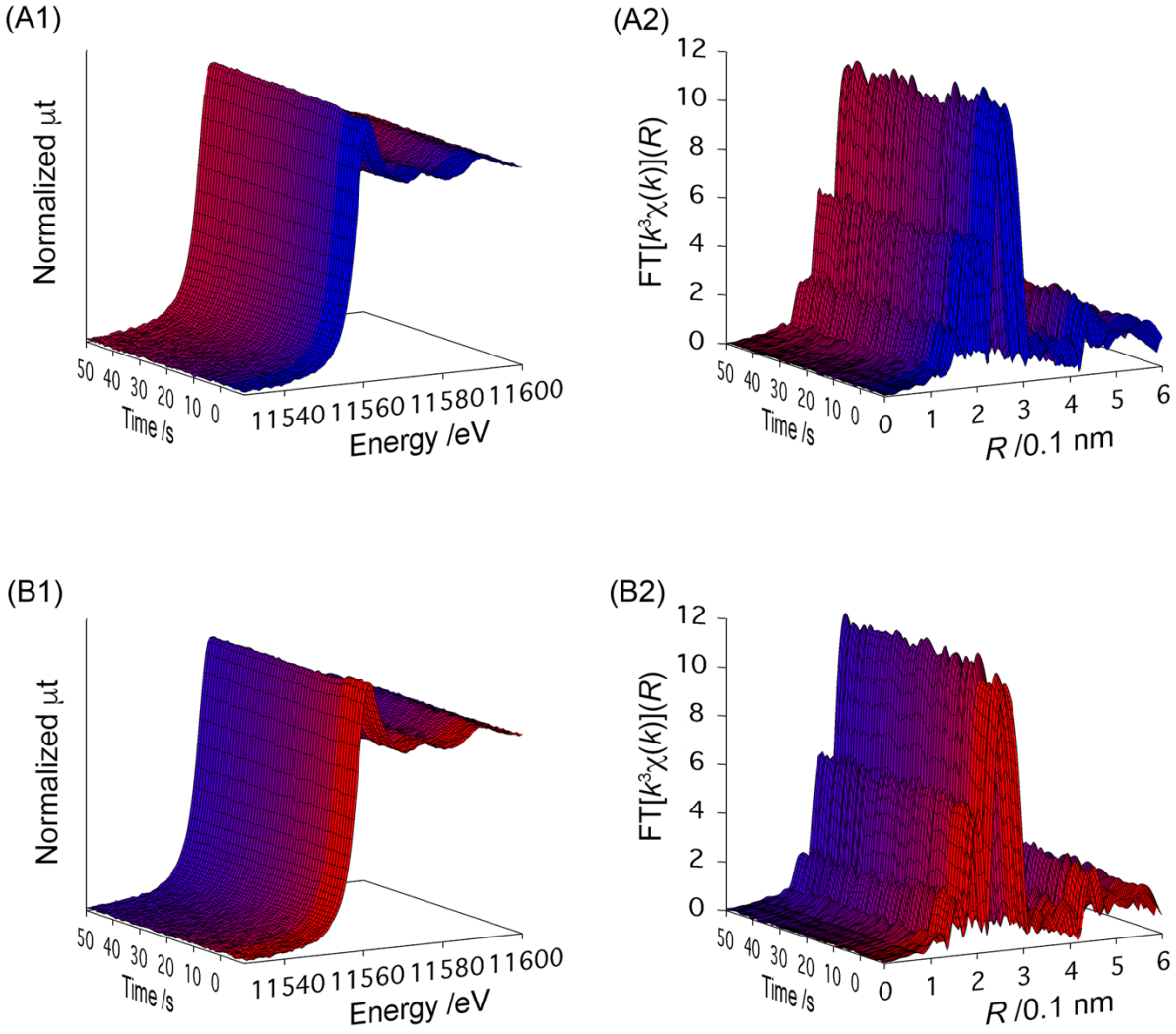

Figure S20. Series of in situ time-resolved Pt L_{III}-edge QXAFS spectra for Pt/C in MEA after 17k ADT cycles. (1) Series of in situ time-resolved Pt L_{III}-edge XANES spectra and (2) series of in situ time-resolved Pt L_{III}-edge k^3-weighted EXAFS Fourier transforms at k = 30–130 nm^{-1} for voltage cycling of (A) 0.4 → 1.0 V and (B) 1.0 → 0.4 V in N_2.

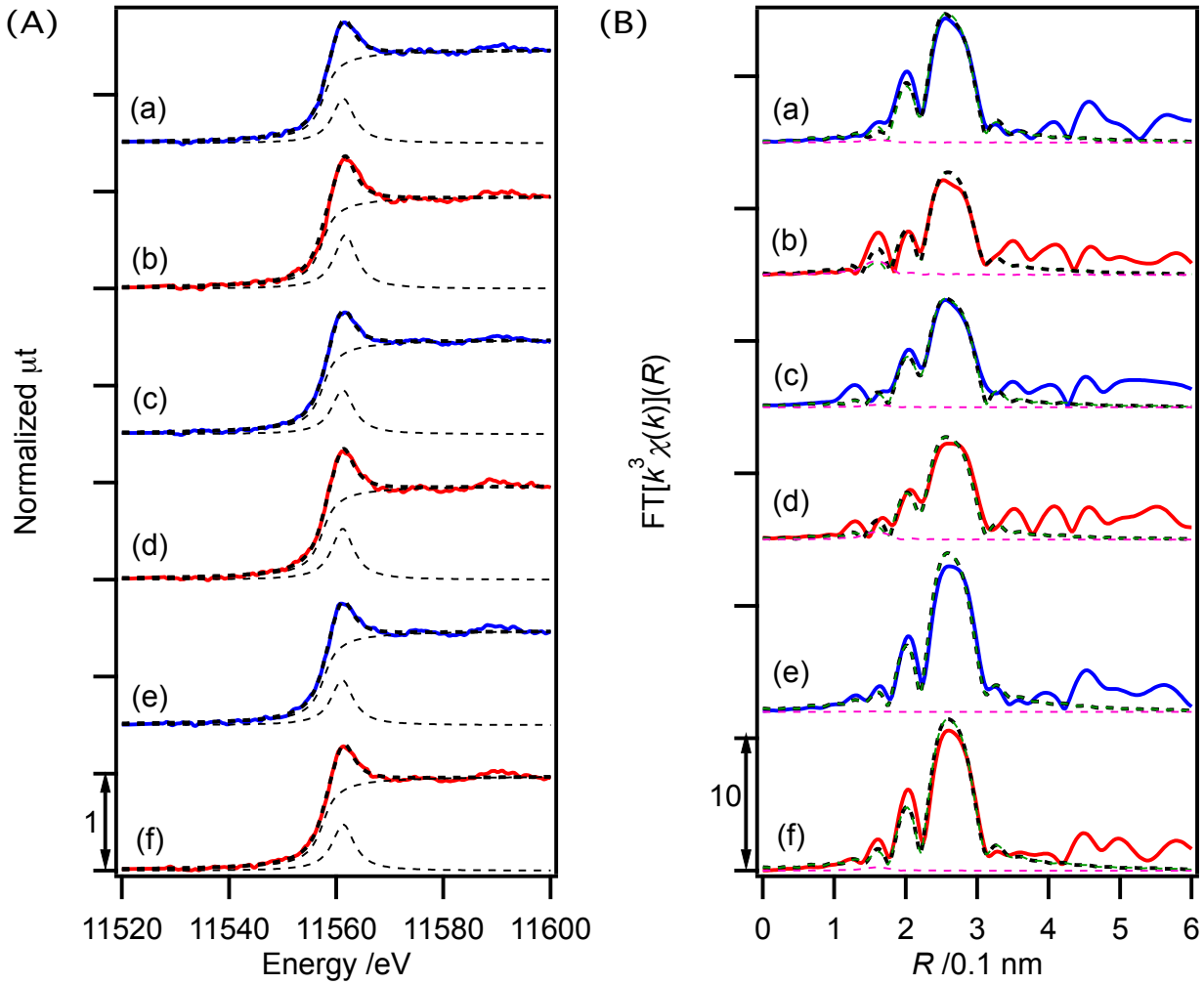

Figure S21. Examples of the curve-fitting analysis of (A) time-resolved Pt L_{III}-edge XANES and (B) time-resolved k^3-weighted EXAFS Fourier transforms for Pt/C. (a) t = 0 s, 0.4 → 1.0 V, in as-prepared MEA, (b) t = 0 s, 1.0 → 0.4 V, in as-prepared MEA, (c) t = 0 s, 0.4 → 1.0 V, in MEA after 2k ADT, (d) t = 0 s, 1.0 → 0.4 V, in MEA after 2k ADT, (e) t = 0 s, 0.4 → 1.0 V, in MEA after 17.5k ADT, (f) t = 0 s, 1.0 → 0.4 V, in MEA after 17.5k ADT. Bold blue and red lines: observed data; black dashed lines in (A): curve-fitted data; green and pink dashed lines in (B): curve-fitted data of Pt-Pt and Pt-O, respectively.

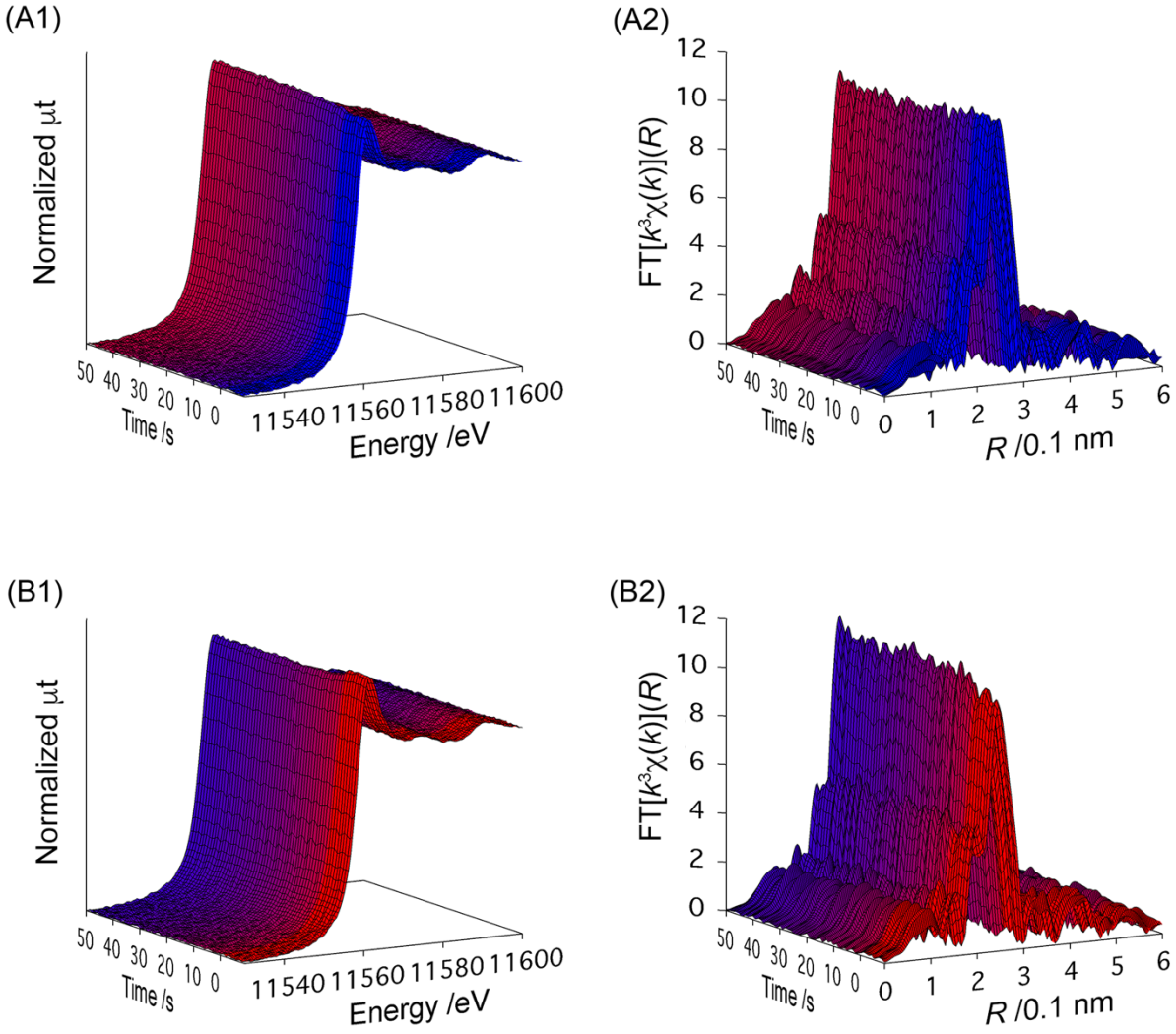

Figure S22. Series of in situ time-resolved Pt L_{III}-edge QXAFS spectra for Pt_3Co/C in MEA after 5k ADT cycles. (1) Series of in situ time-resolved Pt L_{III}-edge XANES spectra and (2) series of in situ time-resolved Pt L_{III}-edge k^3-weighted EXAFS Fourier transforms at k = 30–130 nm^{-1} for voltage cycling of (A) 0.4 → 1.0 V and (B) 1.0 → 0.4 V in N_2.

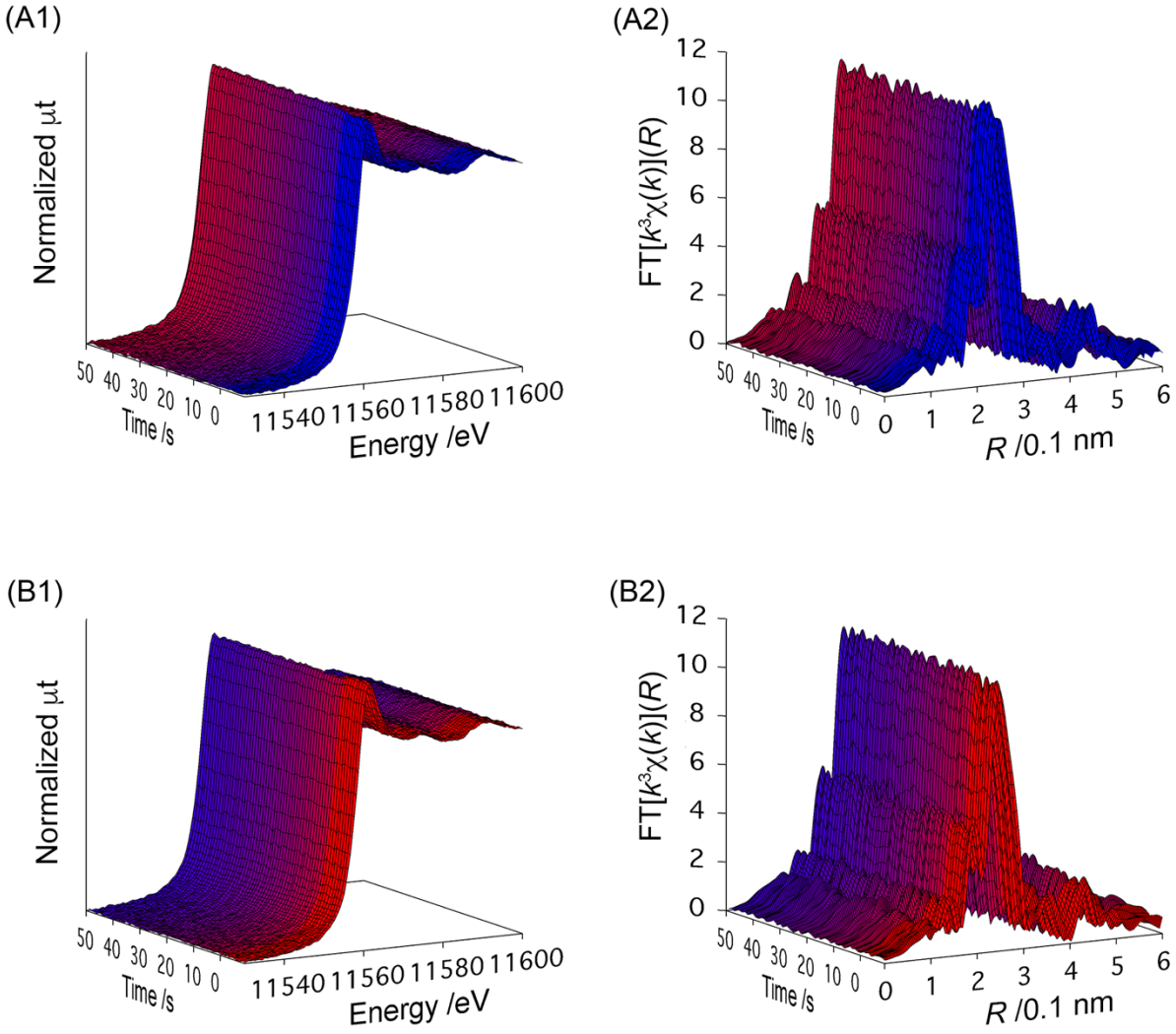

Figure S23. Series of in situ time-resolved Pt L_{III}-edge QXAFS spectra for Pt_3Co/C in MEA after 10k ADT cycles. (1) Series of in situ time-resolved Pt L_{III}-edge XANES spectra and (2) series of in situ time-resolved Pt L_{III}-edge k^3-weighted EXAFS Fourier transforms at k = 30–130 nm^{-1} for voltage cycling of (A) 0.4 → 1.0 V and (B) 1.0 → 0.4 V in N_2.

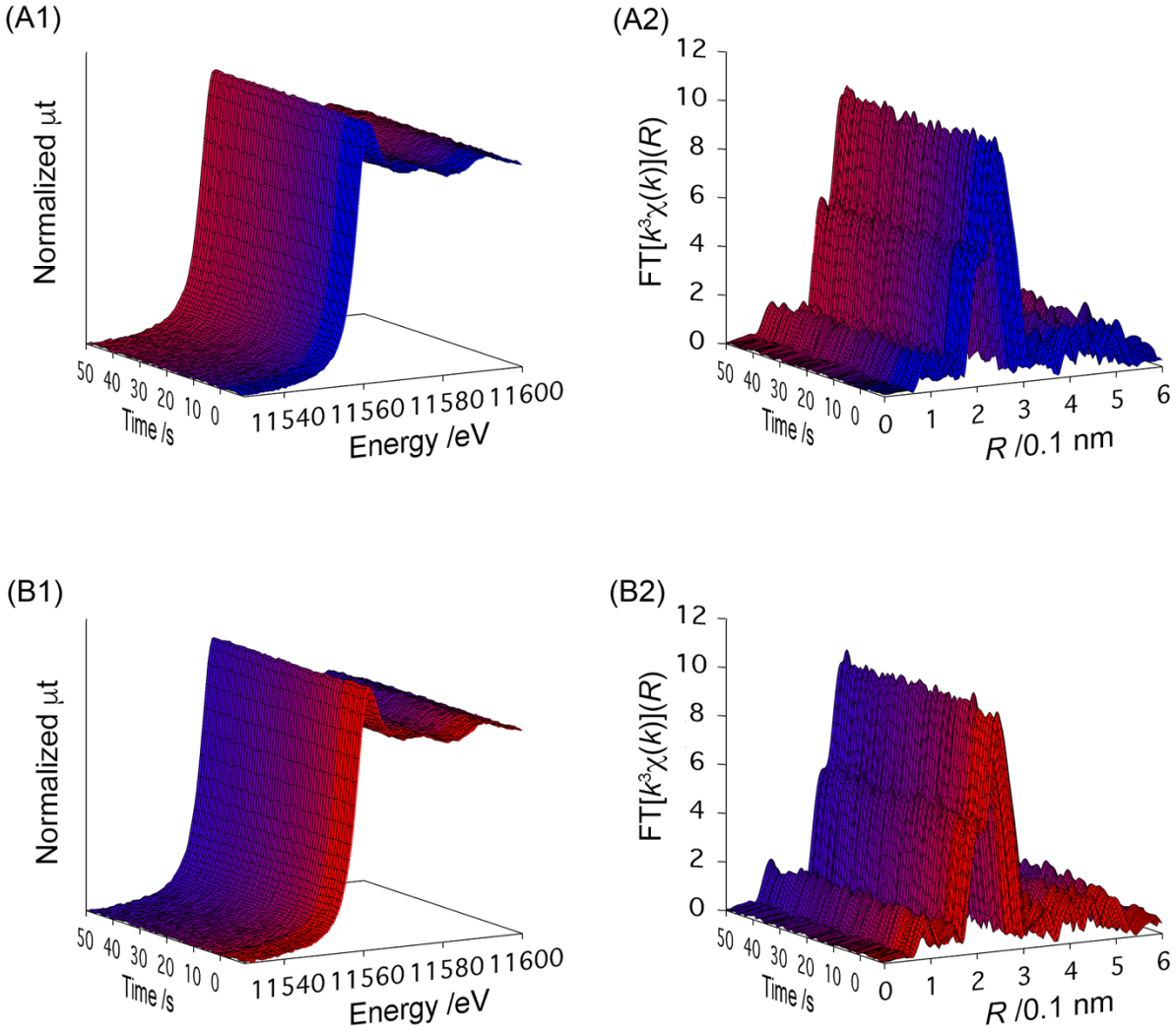

Figure S24. Series of in situ time-resolved Pt L_{III}-edge QXAFS spectra for Pt_3Co/C in MEA after 20k ADT cycles. (1) Series of in situ time-resolved Pt L_{III}-edge XANES spectra and (2) series of in situ time-resolved Pt L_{III}-edge k^3-weighted EXAFS Fourier transforms at k = 30–130 nm^{-1} for voltage cycling of (A) 0.4 → 1.0 V and (B) 1.0 → 0.4 V in N_2.

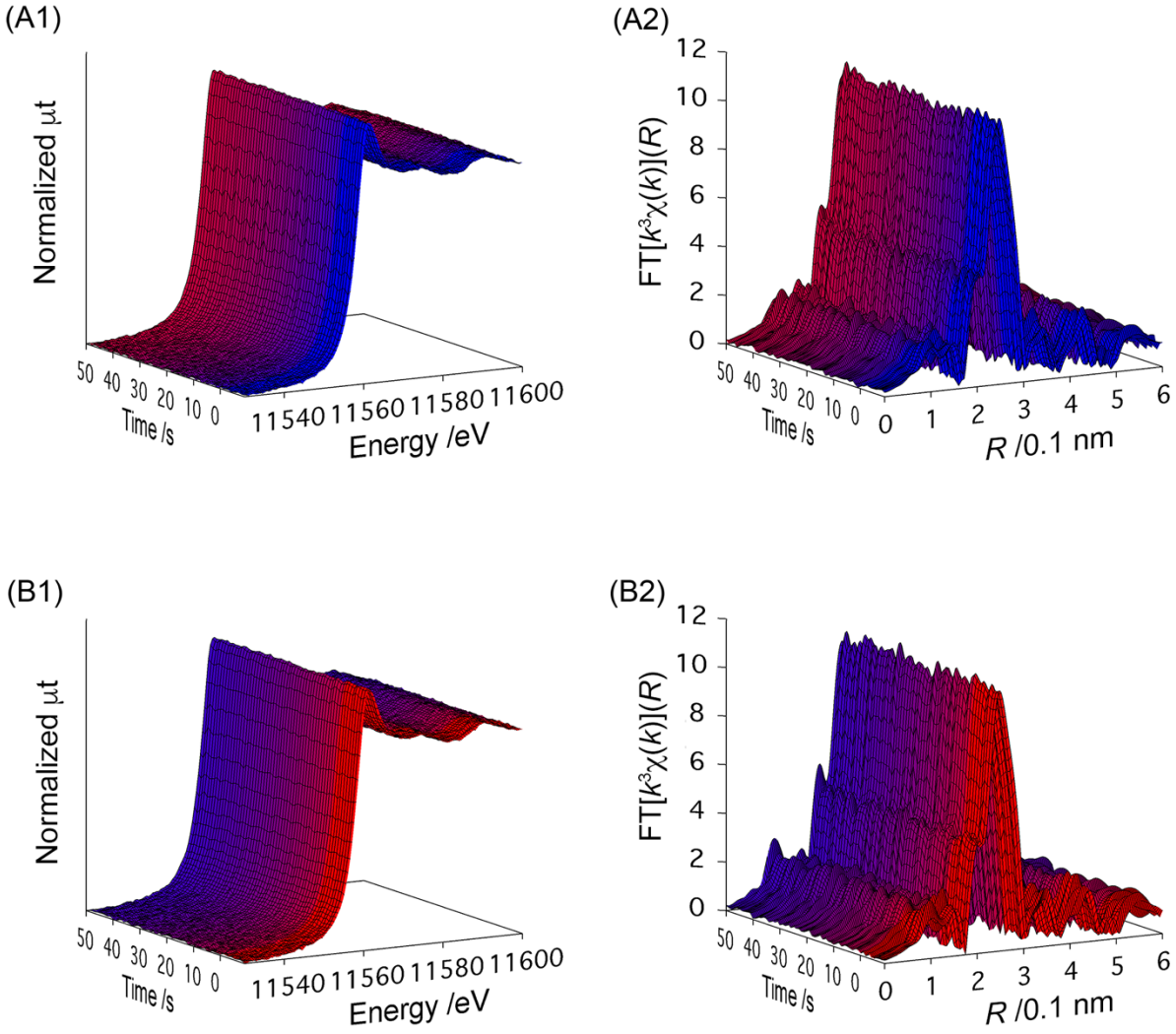

Figure S25. Series of in situ time-resolved Pt L_{III}-edge QXAFS spectra for Pt_3Co/C in MEA after 30k ADT cycles. (1) Series of in situ time-resolved Pt L_{III}-edge XANES spectra and (2) series of in situ time-resolved Pt L_{III}-edge k^3-weighted EXAFS Fourier transforms at k = 30–130 nm^{-1} for voltage cycling of (A) 0.4 → 1.0 V and (B) 1.0 → 0.4 V in N_2.

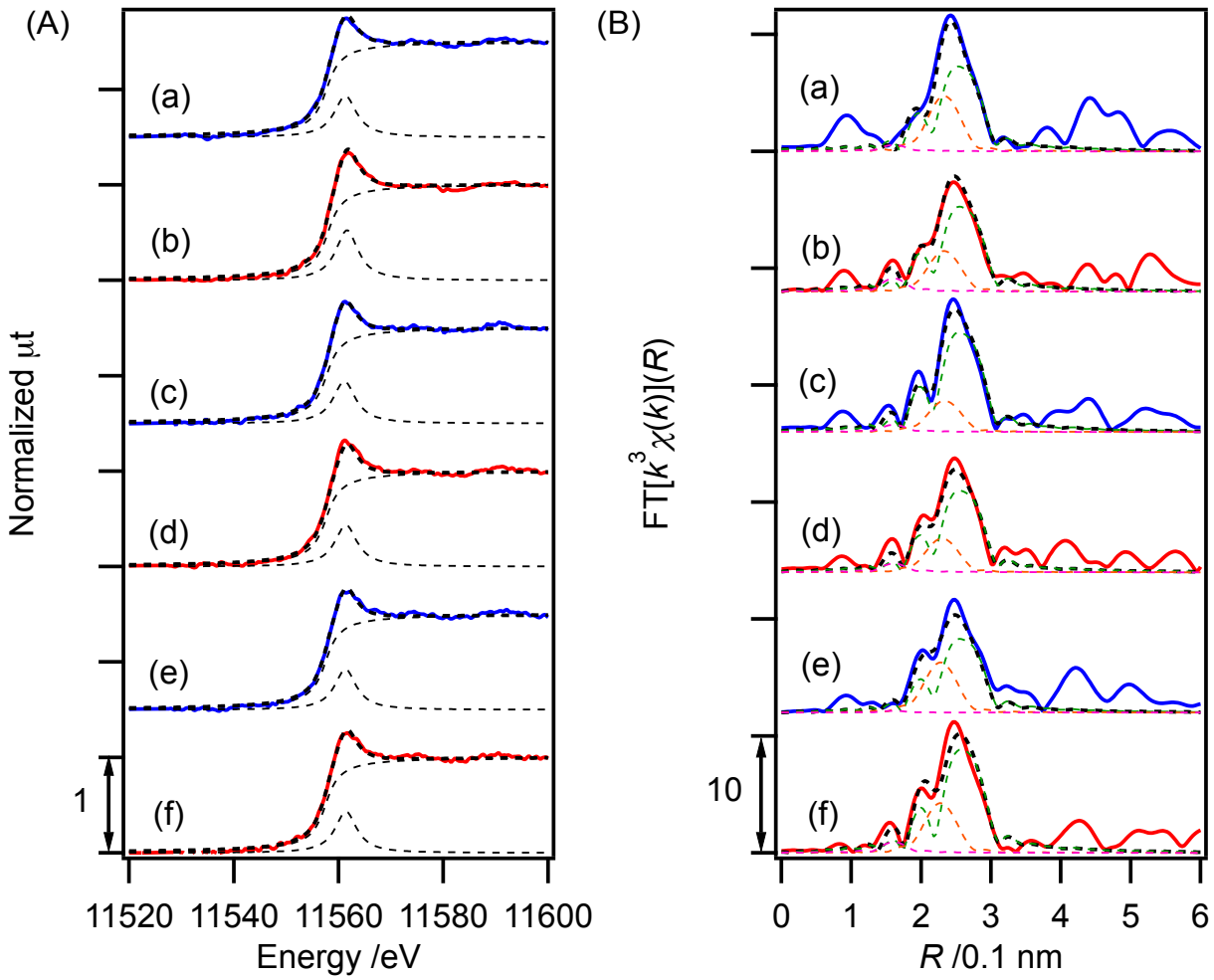

Figure S26. Examples of the curve-fitting analysis of (A) time-resolved Pt L_{III}-edge XANES and (B) time-resolved k^3-weighted EXAFS Fourier transforms for Pt_3Co/C. (a) t = 0 s, 0.4 → 1.0 V, in as-prepared MEA, (b) t = 0 s, 1.0 → 0.4 V, in as-prepared MEA, (c) t = 0 s, 0.4 → 1.0 V, in MEA after 5k ADT, (d) t = 0 s, 1.0 → 0.4 V, in MEA after 5k ADT, (e) t = 0 s, 0.4 → 1.0 V, in MEA after 35k ADT, (f) t = 0 s, 1.0 → 0.4 V, in MEA after 35k ADT. Bold blue and red lines: observed data; black dashed lines in (A): curve-fitted data; green, orange, and pink dashed lines in (B): curve-fitted data of Pt-Pt, Pt-Co, and Pt-O, respectively.

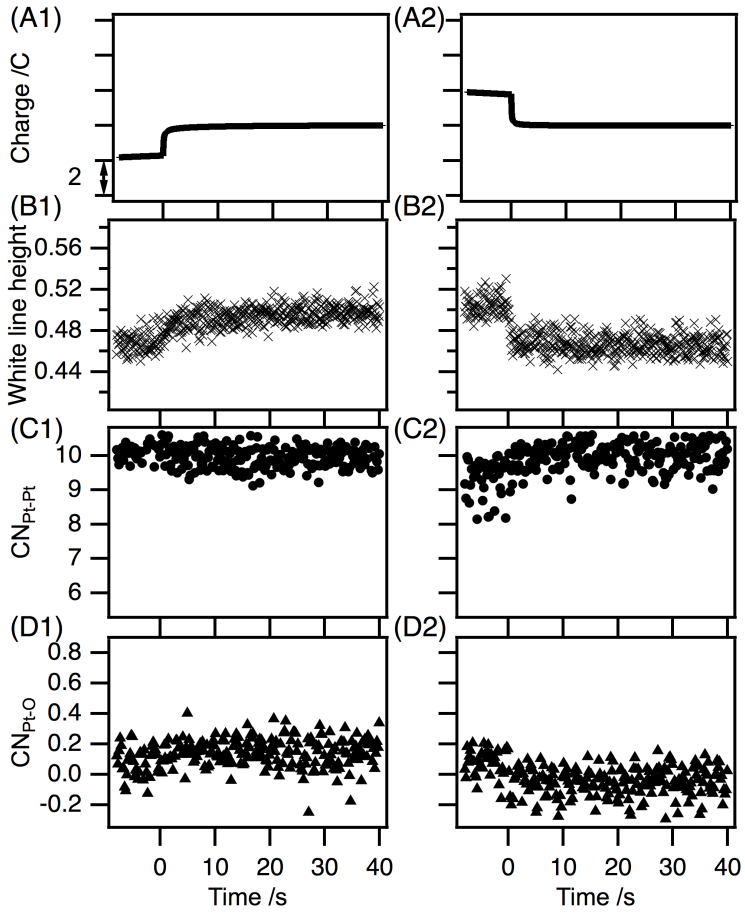

Figure S27. Time profiles of (A) electrochemical charge, (B) Pt L_{III}-edge white line height, (C) CN of Pt−Pt bonds, (D) CN of Pt−O bonds, for the voltage cycling of Pt/C after 35k ADT. (1) 0.4 → 1.0 V; (2) 1.0 → 0.4 V. (×) White line height; (●): CN of Pt-Pt; and (▲) CN of Pt-O.

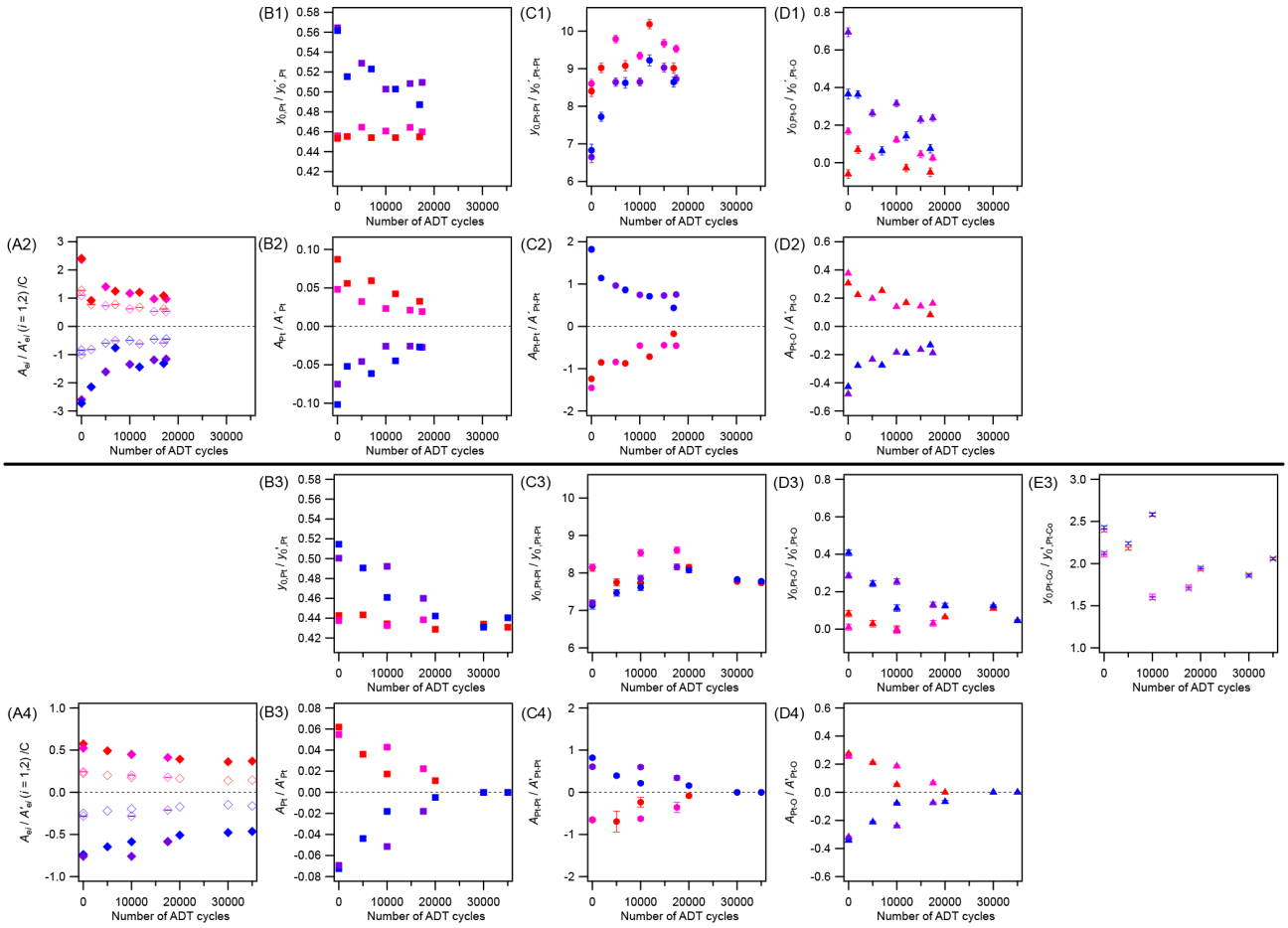

Figure S28. Plots of structural kinetic parameters for Pt/C and Pt_3Co/C in the MEAs for the voltage cycling during ADT. (1,3) Baseline value (y_0 /y_0´) and (2,4) variation range (A /A´) of (A: 1 (◆) and 2 (◇)) electrochemical charge, (B: ■) Pt L_{III}-edge white line height, (C: ●) CN of Pt-Pt bonds ($CN_{Pt\text{-}Pt}$), and (D: ▲) CN of Pt-O bonds ($CN_{Pt\text{-}Pt}$). (red and pink symbols) 0.4 → 1.0 V; (blue and purple symbols) 1.0 → 0.4 V, respectively (different colors shows data in different MEAs).

References

(1) Borup, R.; Meyers, J.; Pivovar, B.; Kim, Y. S.; Mukundan, R.; Garland, N.; Myers, D.; Wilson, M.; Garzon, F.; Wood, D.; Zelenay, P.; More, K.; Stroh, K.; Zawodzinski, T.; Boncella, J.; McGrath, J. E.; Inaba, M.; Miyatake, K.; Hori, M.; Ota, K.; Ogumi, Z.; Miyata, S.; Nishikata, A.; Siroma, Z.; Uchimoto, Y.; Yasuda, K.; Kimijima, K.; Iwashita, N. *Chem. Rev.* **2007,** *107,* 3904-3951.

(35) Sekizawa, O.; Uruga, T.; Tada, M.; Nitta, K.; Kato, K.; Tanida, H.; Takeshita, K.; Takahashi, S.; Sano, M.; Aoyagi, H.; Watanabe, A.; Nariyama, N.; Ohashi, H.; Yumoto, H.; Koyama, T.; Senba, Y.; Takeuchi, T.; Furukawa, Y.; Ohata, T.; Matsushita, T.; Ishizawa, Y.; Kudo, T.; Kimura, H.; Yamazaki, H.; Tanaka, T.; Bizen, T.; Seike, T.; Goto, S.; Ohno, H.; Takata, M.; Kitamura, H.; Ishikawa, T.; Yokoyama, T.; Iwasawa, Y. *J. Phys. Conf. Ser.* **2013,** *430,* 012020.